



Journal of the Geological Survey of Brazil

The volcanogenic perspective on the world-class Chapada Cu-Au deposit in Central Brazil revisited

Sérgio Luiz Martini^{1*} 

¹Independent geologist. Rua Pedro Weingartner 168/601, Rio Branco – Porto Alegre – Brazil, CEP: 90430.140

Abstract

The Chapada deposit, located in the Neoproterozoic intraoceanic Mara Rosa Magmatic Arc, is a low-grade, world-class metallic concentration with a minimum endowment of 3.78 Mt Cu plus 7.76 Moz Au. Ore consists of pyrite-chalcopyrite disseminated mainly in early Neoproterozoic biotite-rich schist pertaining to a mafic-dominated volcanic-sedimentary sequence intruded by 884 to 865 Ma-old gneissic diorite-tonalite. The deposit was metamorphosed and isoclinally folded in a fold-and-thrust system under upper amphibolite facies conditions at 760-730 Ma, and underwent further metamorphism and deformation under greenschist facies conditions at 630-600 Ma, leading to difficulties to unravel its nature. Pre-metamorphic hydrothermal alteration includes an ore-bearing potassic biotitic core with haloes of phyllic (muscovite-pyrite-rich), argillic (quartz-muscovite-kyanite-bearing), advanced argillic (quartz-kyanite-rich), and propylitic (amphibole-epidote-bearing) alteration. Based on these features – along with the identification of A- and D-type veinlets, and sulfur isotope results close to zero per mil – Chapada has been considered a porphyry-type deposit. This conception, from 1986, has gained general acceptance, whereas another early proposition, from 1989, of a volcanogenic nature for Chapada, has been practically dismissed. Nonetheless, the geologic setting of Chapada is permissive for volcanogenic deposits. Considering this, the volcanogenic perspective on Chapada is re-evaluated here. The exercise has been carried out by scrutinizing essential attributes of volcanogenic deposits searching for features comparable to those of Chapada. The outcome is that the evidence leading to the acceptance of the porphyry model for Chapada applies equally to support a volcanogenic interpretation. This situation probably reflects a shallow-crustal, sub-volcanic environment, where both deposit types share attributes as, e.g., epithermal-style high-sulfidation alteration. The picture obtained allows for the working hypothesis that a volcanogenic relationship exists between epidote-rich amphibolite source rocks in the west, and quartzitic cap rocks in the east, of Chapada to produce disseminated ore, with accompanying K-Al-Si-propylitic alterations and a magnesian zone made up of early-recognized gedrite-staurolite rocks. The situation envisaged is that ore deposition occurred in sub-seafloor conditions from a poorly focused hydrothermal upflow discharge of fluids from a convective system with magmatic contribution. The volcanogenic model for Chapada is reinforced by the recent discovery of active submarine volcanogenic Cu-Au systems with high-sulfidation silica-alumina alteration, by the incidence of equally high-alumina alteration in the 40 km-distant VMS-affiliated Zacarias Au-Ag-Ba deposit, and by the localization of the deposit in a regional zone of alteration, with a suggested exhalative contribution, that seems to fit the concept of favorable, or equivalent, ore horizon.

Article Information

Publication type: Research papers
Received 9 September 2020
Accepted 7 April 2021
Online pub. 26 May 2021
Editor: E.L. Klein

Keywords:
Chapada,
volcanic-associated,
typological attributes,
hydrothermal alteration,
exhalite

*Corresponding author
Sérgio Luiz Martini
E-mail address: martini.s@uol.com.br

1 Introduction

The Neoproterozoic juvenile Mara Rosa Arc constitutes the northern segment of the Goiás Magmatic Arc that evolved in the Tocantins Province between the Amazonian, São Francisco and Paraná cratons in the Neoproterozoic, during the development of the Brasileiro / Pan African orogeny,

with attending high-grade peak metamorphism and severe deformation (Pimentel et al. 1997, 2000, 2004). In terms of mineralization, the Mara Rosa Arc contains three long-known and differently-endowed metallic deposits hosted in the Mara Rosa metavolcanic-sedimentary sequence, namely, Zacarias (Au-Ag-Ba, small), Posse (Au, medium-sized) and Chapada (Cu-Au, world-class, low-grade, with resources of 2.84 Mt



Cu @ 0,24% plus 5,15 Moz Au @ 0,14 g/t, with additional historical production from 2007 to ending June 2019 of 0.94 Mt Cu @ 0.38% and 2.61 Moz Au @ 0.33 g/t; Moore et al. 2019). To these, it should be added the relatively recently-defined Chapada's satellite Suruca, distant 5 km to the NE, with Cu-Au resources of 0.11 Mt Cu @ 0.15% plus 0.5 Moz Au @ 0.22 g/t, and gold-only resources of 2.5 Moz Au @ 0.53 g/t; Moore et al. 2019). Zacarias and Posse are both deposits of settled classification. The former is a gold-rich volcanogenic deposit (Arantes et al. 1991; Pöll 1994) and the latter is mesothermal, orogenic gold (Palermo 1996a; Palermo et al. 2000), though originally also considered volcanogenic as well (Angeiras et al. 1988), whereas Suruca was formerly modeled as an intermediate-sulfidation epithermal deposit (Silva et al. 2011), but now is considered a skarn (Miranda et al. 2018, Moore et al. 2019).

Chapada, in contrast, has been variously classified over time. In the eighties, it was considered either a wall rock-hosted porphyry (Richardson et al. 1986) or a volcanogenic deposit (e.g., Silva and Sá 1988; Kuyumjian 1989a). This latter model persisted in the nineties (Kuyumjian 1991, 1995, 1998a) but was dropped in the turn of the century. It has since been classified as porphyry-epithermal (Kuyumjian 2000; Ramos Filho et al. 2005), orogenic (Ramos Filho et al. 2003), as partly porphyry partly orogenic or intrusion-related (Oliveira 2009; Kuyumjian et al. 2010; Oliveira et al. 2014, 2016) and as a Cu-Au porphyry system (Miranda et al. 2018; Moore et al. 2019), with the porphyry model becoming eventually predominant. Evidently, this diversity of interpretation reflects to a good extent the fact that Chapada – recognized almost unanimously as pre-metamorphic – underwent severe metamorphism and deformation in connection with the development of the Mara Rosa Arc, making difficult the unravelling of its original geologic and metallogenic setting. However, despite the general acceptance of the porphyry model nowadays for Chapada and the complicated geologic setting, the deposit does exhibit a number of features that can be ascribed to the volcanogenic model, and this probably influenced the earlier above-mentioned interpretations. Considering these aspects, we decided to re-evaluate the possibility of Chapada fitting or being geologically congruent with the volcanogenic model. The exercise has been carried out through scrutinizing the literature on both the deposit and the model focusing on the concept of typology and type of deposit, as explained below.

2 Methodology: using typology and deposit type as a comparative tool

Typology refers to a systematics governed by morphology and type of mineral deposit is a descriptive model based on this approach. Accordingly, a type of deposit may be taken either as a group of deposits with a significant number of common morphological attributes, or with sufficient features in common with a famous and well-understood 'type example' (Dixon 1981, p. 11; see also Routhier 1963; Eckstrand et al. 1996; Martini 2002; Jébrak and Marcoux 2014). Volcanogenic massive sulfides (VMS), which are at the core of the present exercise, and porphyry copper deposits constitute examples of well-established mineral deposit types. According to Routhier (1980, 1983), a type of deposit is above all an anatomical model, comprising organs, or parts, that appear to have a

functional link, e.g., massive sulfide bodies and subjacent hydrothermal chimneys.

In accordance with the premises above, it is our contention here that - based on the concepts of typology and deposit type - one may find in the literature adequate information to contribute to the elucidation of the geologic nature deposits in general, and, in the present case, of Chapada in particular. This information fortunately has actually been available in a conveniently condensed form through compilation papers on volcanogenic deposits contained in review books such as, inter alia, those edited by the Geologic Survey and the Geological Association of Canada (Hutchinson et al. 1982; Kirkham et al. 1993; Eckstrand et al. 1995; Goodfellow 2007), the Society of the Economic Geologists (Skinner 1981; Hagemann and Brown 2000; Hedenquist et al. 2005) and the British Columbia Geological Survey (e.g., Lefebure and Ray 1995; Lefebure and Höy 1996). Therefore, the essential method used in the present exercise is comparing attributes of Chapada, as per the specific literature exemplified above, with those consecrated by the typology of volcanogenic deposits.

The subject is treated with particular reference to the essential attributes of volcanogenic deposits and their geologic setting as contemplated by comprehensive reviews on this deposit type (e.g., Franklin et al. 2005; Gibson et al. 2007), namely, magmatic heat sources, semi-conformable regional alteration zones, synvolcanic faults, deposit-scale alteration pattern, features of the orebody itself and of associated exhalative products. In the exercise, there is no intention of making comparison with, or checking the merits of, the other above-mentioned models that have been applied to Chapada.

Information on volcanogenic attributes has been extracted from the two above-mentioned reference works with additional material taken mainly from Dubé et al. (2007), Galley et al. (2007), Huston (2000), Franklin (1993, 1996), Franklin et al. (1981), Large (1992), and Poulsen and Hannington (1996). Information on Chapada and environs, in turn, has been obtained mainly from the related sources referred to in the introductory section above, with particular reference to the work authored by Kuyumjian R.M., Richardson S.V., Oliveira C.G., Oliveira F.B. and collaborators, as shown in the reference list. Aspects of each of the essential volcanogenic attributes and their correlation with features of Chapada are addressed and discussed in the following sections.

3 Regional and local geology

3.1 Regional geology

The Chapada Cu-Au deposit in central Brazil is hosted in the Goiás Magmatic Arc, more specifically in its northern portion denominated Mara Rosa Arc, which lies along the NW marginal zone of the Brasília Fold Belt (Fig. 1). This belt constitutes the eastern branch of the Tocantins province, a large Neoproterozoic orogenic system located between the Amazonian and São Francisco cratons and the postulated Paranapanema Craton or Paraná Block, hidden under Phanerozoic cover (Fig. 1, inset). The geologic history of the province initiated with the rifting of the Rodinia paleocontinent at 950-900 Ma and proceeded through collisional events towards the end of the Neoproterozoic that culminated in an early phase of the amalgamation of Gondwana. The Goiás Magmatic Arc in particular generated pre-collisional

magmatism from ca. 910 Ma to 640 Ma, and was subsequently accreted to the Tocantins orogen and to the western margin of the São Francisco Craton towards ca. 600 Ma with the closure of a previous extensive oceanic basin (Valeriano et al. 2004; Pimentel et al. 2000, 2004; Oliveira et al. 2016).

According to Kuyumjian et al. (2010), the Goiás Magmatic Arc itself consists of a collage of intraoceanic island arcs between the Neoproterozoic Amazon and S. Francisco

cratons, and records a long period (900-600 Ma) of plate convergence and magmatic arc formation, including arc-continent and continent-continent collisions. Two main periods of crustal accretion and igneous activity have been recognized in the arc, at ca. 940-800 Ma and 660-600 Ma (Junges et al. 2003; Laux et al. 2005). According to Pimentel et al. (2000, 2004), at ca. 760 Ma the Goiás Arc underwent upper amphibolite facies metamorphism during collision

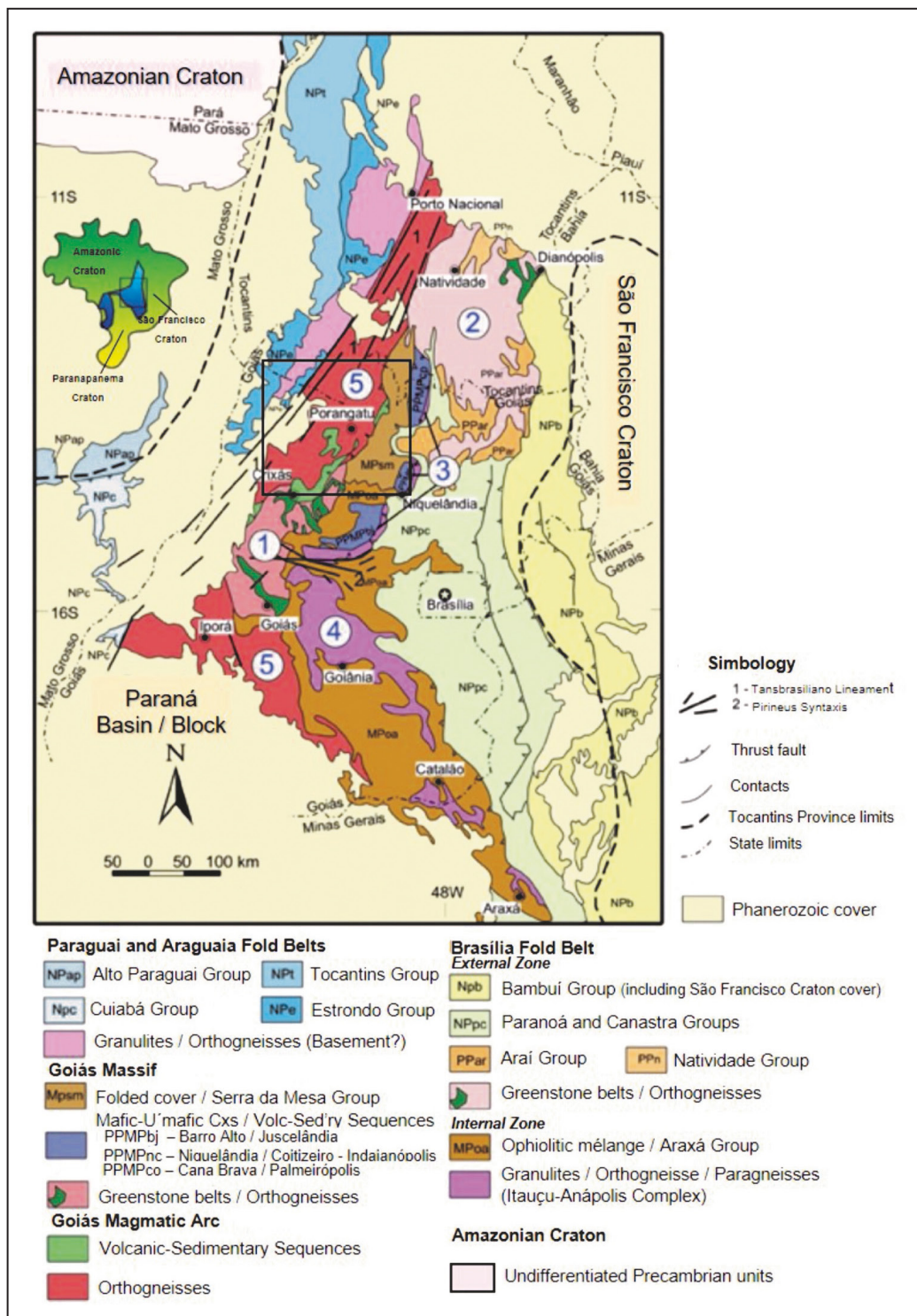


FIGURE 1. Simplified geologic map of the central-eastern part of the Tocantins Province. 1- Archean Crixás-Goiás Block, 2- Paleoproterozoic terranes of Almas-Natividade, 3- Mafic-Ultramafic Complexes, 4- Anápolis-Itaçu Complex, 5- Goiás Magmatic Arc. The inset exhibits the location of the Tocantins Province in relation to the adjacent São Francisco, Amazonian and Paranapanema cratons (modified from Pimentel et al. 2004). Location of Figure 2 covering the Mara Rosa Magmatic Arc and the Chapada region indicated by square area.

between its northern portion, i.e., the Mara Rosa Arc, and the western margin of the São Francisco craton. Moreover, between ca. 630-600 Ma the entire arc was submitted to a second metamorphic episode, in greenschist facies, with the development of extensive N-NE trending shear zones and E-verging thrust faults. Regional uplift and post-collisional bimodal granitic and gabbro-dioritic magmatism ensued, in the 590-560 Ma period. In the southern section of the arc, mafic magmatism occurred between 650-600 Ma, indicating extensional tectonic episodes amidst the general collisional environment. Peraluminous syntectonic granites of 640-615 Ma are also referred to, e.g., in Junges et al. (2003). The final picture is that, by virtue of the erosion level, the arc as a whole consists of a sea of orthogneiss with subordinated strips of volcanic-sedimentary units and dispersed, mostly younger granitic and mafic intrusions.

The Mara Rosa Arc, specifically, shows a general NE-trending structural fabric, being delimited to the NW and SE by the Transbrasiliano strike-slip fault system and the Rio dos Bois thrust-fault system, respectively (cf. Kuyumjian et al. 2010; Oliveira et al. 2016; Fig. 2). The arc can be divided roughly diagonally along a NW-SE thrust zone of the Rio dos Bois system into two domains for which U-Pb zircon data

indicate two individual periods of granitoid arc magmatism, probably reflecting different tectonic environments, (e.g., Junges et al. 2003). The older event is recorded SE of the mentioned thrust zone. It spans from 900 to 800 Ma and took place in an intra-oceanic island arc setting. The younger event developed NW of the former from ca. 670 to 600 Ma most probably in a Cordilleran magmatic arc setting. Thus, the Mara Rosa Arc as a whole underwent two distinct periods of tonalitic magmatism and crustal accretion. Associated to the mentioned oceanic and continental arc settings, respectively, are the Mara Rosa and Santa Terezinha volcanic-sedimentary sequences.

The Mara Rosa metavolcanic-sedimentary sequence hosts the main metallic deposits of the Mara Rosa Arc. It occurs in a belt approximately 100 km x 25 km along the SE portion of the arc, in contact with dioritic-tonalitic orthogneisses to the NE and SW, and encompassing the Chapada-Mara Rosa region (cf. Fig. 2). U-Pb zircon data return ages of 908 to 884 Ma and 885 to 856 Ma for the protoliths of these two units, respectively (cf. section 5.1). This SE portion of the Mara Rosa Arc evolved as a system of intra-oceanic island arcs characterized by calc-alkaline volcanic rocks and plutonic gneissic complexes. The orthogneisses are chemically very

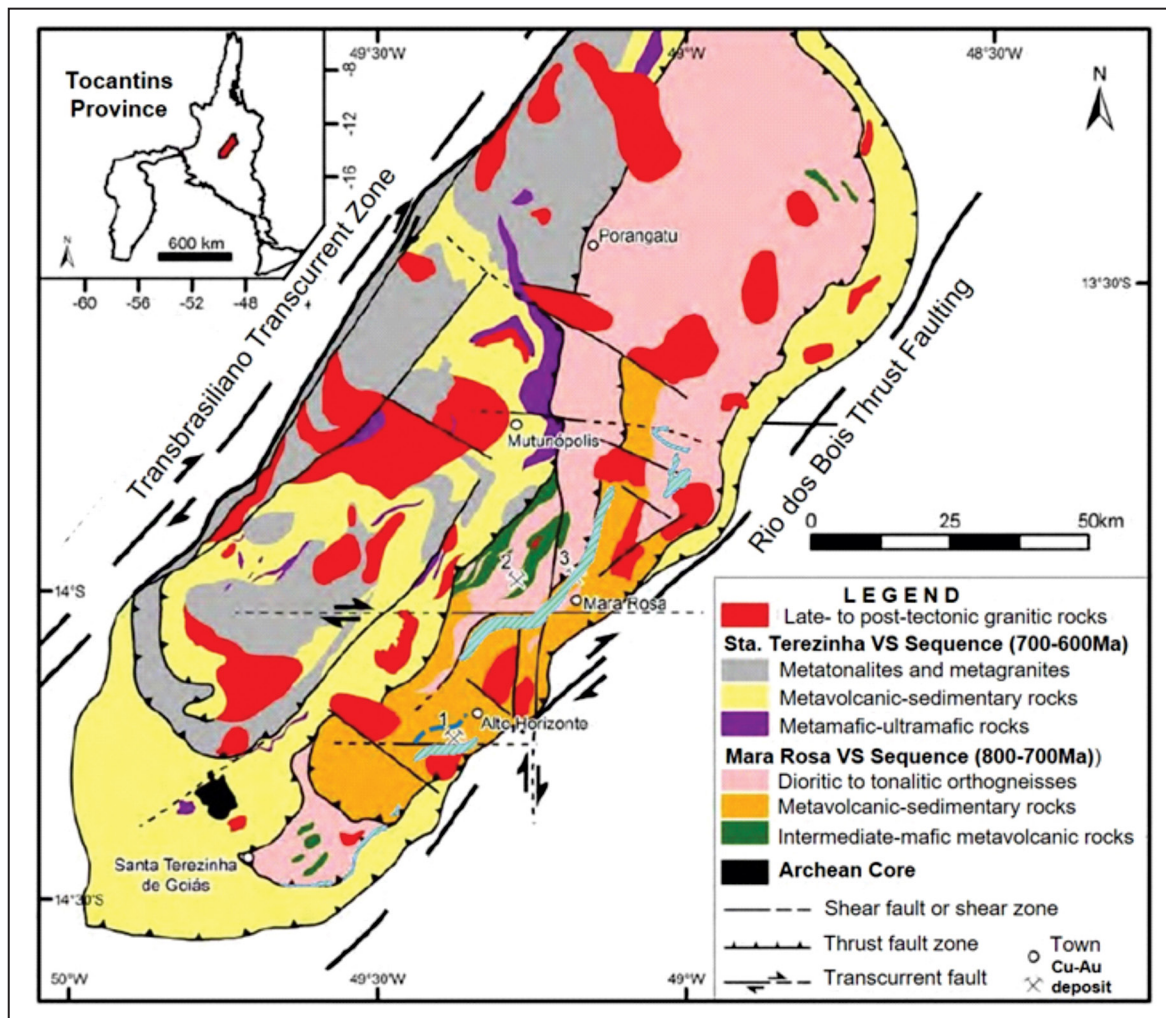


FIGURE 2. Geologic map of the Mara Rosa Magmatic Arc showing in particular the Mara Rosa (900-800 Ma) and the Santa Terezinha (670-600 Ma) metavolcanic-sedimentary units as well as the copper and/or gold deposits (1- Chapada, 2- Zacarias, 3- Posse, modified from Oliveira et al. 2014). The regional kyanitite unit (lined blue) and the zone of epidote-rich amphibolite just west of Chapada (blue-gray line) have been added on schematically (cf. Oliveira et al. 2016 and Kuyumjian 1991, respectively).

primitive, similar to M-type granitoids of immature island arcs (Viana et al. 1995). Some mafic volcanic rocks are tholeiitic, rich in Mg, Ni and Cr, similar to boninites (Palermo 1996b), perhaps implying episodes of extension in the arc system. In the Chapada area, quartz-garnet amphibolites and clinopyroxene amphibolites have chemical characteristics of modern arc calc-alkaline basaltic andesites and back-arc tholeiitic basalts, respectively, suggesting a tectonic development as an arc-back arc pair (Kuyumjian 1989a, 1991, 1994). Additionally, detrital metasedimentary rocks of the arc, such as feldspathic garnet schist and fine-grained biotite gneiss, show isotopic data indicating that they originated from the erosion of arc rocks and deposited away from any continental source areas, probably in an intra-oceanic setting (Pimentel et al. 2000). According to Junges et al. (2002), isotopic data and mineral chemistry of metasedimentary rocks of the Mara Rosa sequence indicate two metamorphic events, one at ca. 760-730 Ma and ca. and the other at ca. 630-600 Ma, at lower P-T condition than the former. The older metamorphic event is interpreted preliminarily as the result of the accretion of island arc terranes to the western edge of the orogen and the younger event, as the result of final ocean closure and continental collision between the Amazon and São Francisco continents.

The Mara Rosa sequence is made up of metabasalt, intermediate to felsic metatuff, metaultramafic rock, fine-grained metagreywacke, quartzite, garnet-mica schist, metachert, iron-formation and gondite accompanied by a variety of metapelitic/psammitic rocks and regionally extensive rock types interpreted to be of hydrothermal origin. The latter consist mainly of kyanites, pyritic kyanite-sillimanite-muscovite quartzites and quartz schists (e.g., Palermo et al. 2000; Kuyumjian et al. 2010). The peraluminous kyanite-bearing rocks form lenses that occur approximately along strike almost continuously for ca. 100 km from the SW of Chapada to the NE of the Mara Rosa town (Arantes et al. 1991; Oliveira et al. 2016; Fig. 2). Additionally, epidotized amphibolites have been mapped over a minimum area of ca. 50 km x 4 km, located west of the Chapada deposit, with the more epidote-rich rocks, with up to 40% epidote, and banded epidotes forming a ca. 0.5-1.0 kilometer-wide and several kilometers-long belt immediately west of the deposit (cf. Kuyumjian 1989a, b, 1991, 1998a; Figs. 2 to 4 and sections 5.2 and 5.6). The Mara Rosa sequence contains also small elongate bodies of mylonitized granites some of which were formerly interpreted as felsic metavolcanic rocks. At the Posse mine, one of these bodies showed a protolithic U-Pb zircon age 862 ± 8 Ma with U-Pb titanite dating indicating age of ca. 630 Ma for the metamorphism (Viana et al. 1995; Palermo et al. 2000; Pimentel et al. 2000).

The Mara Rosa sequence was initially deformed and metamorphosed under amphibolite-facies conditions at ca. 760-730 Ma, as quoted above, with attending isoclinal folding (D_n). Subsequently, it underwent deformation (D_{n+1}) and retrograde greenschist metamorphism during SE-oriented thrusting over pre-Neoproterozoic units in the Brasiliano orogeny at ca. 610 Ma. The Chapada Cu-Au deposit is hosted in the Mara Rosa sequence and lies near the SE border of the arc. (Fig. 2).

The Santa Terezinha sequence as represented south of Chapada consists dominantly of metapelites of low metamorphic grade with sparse mafic and felsic metavolcanic

intercalations and with associated metatonalitic-granitic gneissic rocks. One of the felsic volcanic units of the sequence shows a U-Pb zircon age of 661 ± 7 Ma (Dantas et al. 2001).

The late- to post-tectonic granitic intrusions of the Mara Rosa Arc constitute large high-K calc-alkaline batholiths and lesser mafic, gabbro-dioritic stocks. The age of this bi-modal magmatism is 590-560 Ma. It is interpreted as associated with the final uplift and collapse of the Brasiliano Orogen (Pimentel et al. 2000). Besides this, coarse-grained amphibolites with U-Pb zircon ages of 638 ± 2 Ma and 603 ± 2 Ma are reported by Junges et al. (2003). They are interpreted as representing intrusion emplaced during extensional episodes of the generally compressive history of the belt (Pimentel et al. 2000, 2004).

3.2 Local geology

The geology of the Chapada deposit area and environs is dealt with here with specific reference to the recent geologic maps presented by Kuyumjian et al. (2010) and Oliveira et al. (2016).

The map in Kuyumjian et al. (2010) (Fig. 3) shows essentially NE-trending alternating zones of amphibolite/amphibole schist and sericite-muscovite-quartz-feldspar-kyanite-biotite-rich schist with lenses of kyanite-sericite-biotite-rich quartzite that in part align as if they conformed to a stratigraphic horizon. The kyanite quartzite, peculiarly, is positioned stratigraphically above late-tectonic tonalite stocks.

The ore host rocks are described as a variety of schists associated with magnetite-biotite gneisses and amphibolites. Main rock types and rock association are muscovite-biotite schists, constituting 60% of the total host rocks, hornblende-anthophyllite-gedrite schists, an association of kyanite-staurolite-amphibole-garnet-biotite-muscovite schist, feldspathic kyanite-epidote-muscovite-biotite schist and metachert, and an association of pyrite-bearing kyanite, quartz-kyanite, kyanite quartzite and kyanite-muscovite-quartz schist not strictly mineralized in copper, but locally rich in gold. Zones of sericitization and chloritization associated with the mineralization are interpreted to be represented by magnetite-pyrite-quartz-sericite schists and staurolite-gedrite-anthophyllite-rich rocks, respectively. Interestingly, no mention is made by Kuyumjian et al. (2010) to epidote-rich amphibolites and epidotes that were previously mapped by Kuyumjian (1989a, 1991, 1998a) (cf. sections 5.2 and 5.6 ahead).

The ore deposit consists of disseminated pyrite, chalcopyrite and magnetite with feldspathic biotite schist being the most important ore-bearing rock of the deposit, hosting approximately 80% of the ore, with amphibolite and muscovite schist accounting for 10% each, and feldspathic quartzite hosting less than 1% (Richardson et al. 1986). However, according to Oliveira et al. (2004), gedrite-anthophyllite schist instead of amphibolite hosts 10% of the ore and, additionally, a silicified zone forms a subordinate portion of the deposit.

Oliveira et al. (2016) in turn present a more detailed map of the Chapada deposit (Fig. 4), with emphasis on hydrothermally altered rocks, which consist of biotite-rich schist for potassic alteration, muscovite- and quartz-rich schist for phyllic alteration, kyanite- and muscovite-rich schist for argillic alteration, quartzite and kyanite for advanced argillic alteration, and amphibole- and epidote-rich rocks for

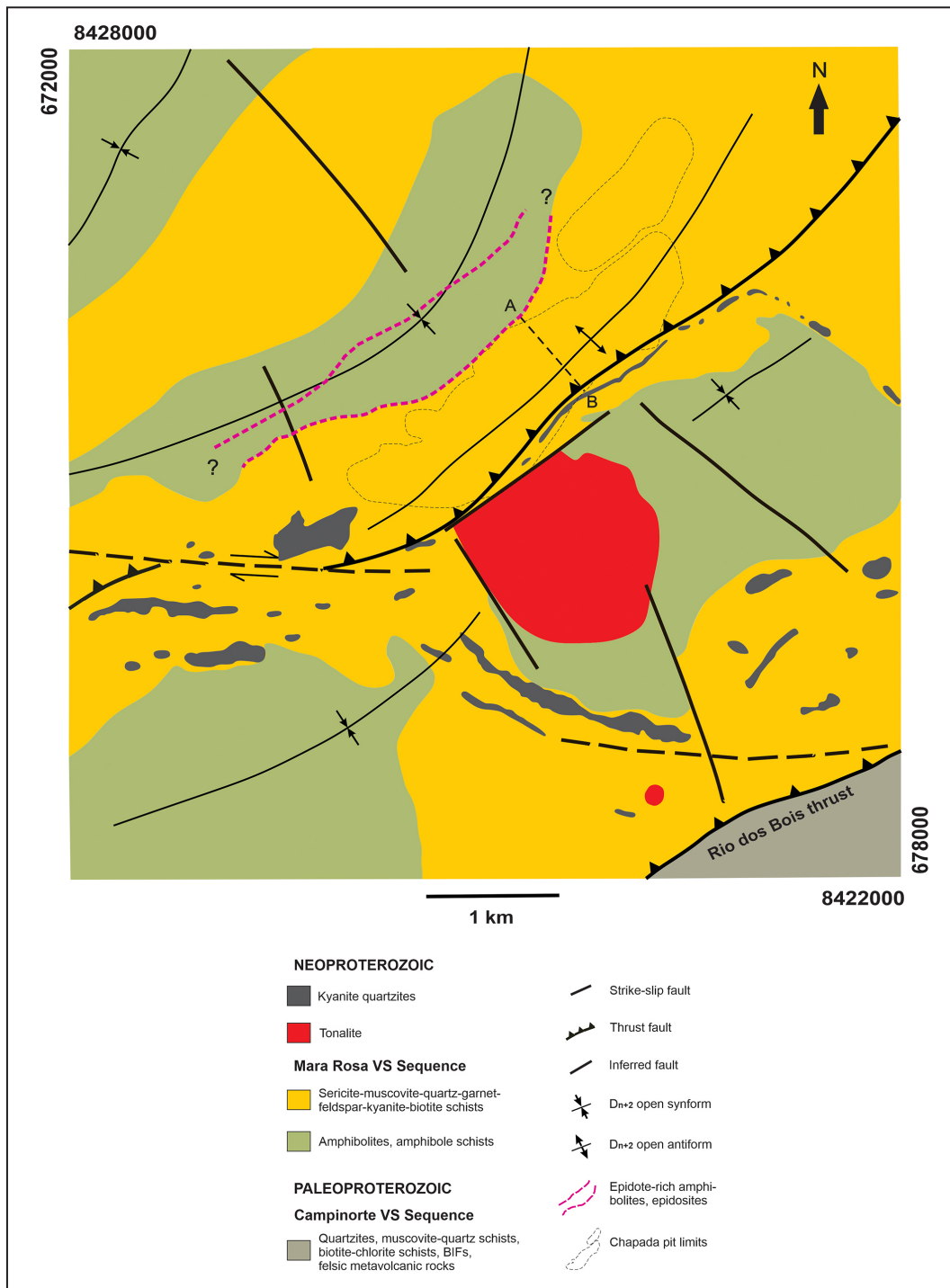


FIGURE 3. Geologic map of the Chapada deposit environs (from Kuyumjian et al. 2010). Approximate location of epidote-rich amphibolite and epidosite shown by red traced line (from Kuyumjian 1989a, 1991, 1998a). Cross-section A-B is presented as Figure 11 in section 5.4.

propylitic alteration. Phyllic alteration is widespread whereas lesser acid-intermediate metavolcaniclastic rocks and hydrothermal tectonites represented by amphibole schists are also referred to. Unmineralized tonalitic to dioritic gneisses representing early Neoproterozoic intrusive rocks are also prominent southeast and south of the deposit.

The Chapada composite orebody is centered on the potassic alteration zone and lies roughly along a thrust-fault contact between a massive bank of amphibolite to the northwest and the above-mentioned widespread phyllic alteration zone (muscovite- and kyanite-rich schist). This agrees in a sense

with Kuyumjian (1989a, 1998a) who shows the deposit lying along the contact between the Eastern and Central belts of the Mara Rosa sequence represented, respectively, by an epidote amphibolite-dominated unit and a metavolcanic-sedimentary unit of metasandstone, feldspathic biotite schist, staurolite-kyanite-mica schist, garnet-mica schist, amphibole schist, felsic metavolcanic rocks, intermediate metatuffs, banded iron-formation and metachert.

According to Oliveira et al. (2016), the mineralized or sulfide-rich ore host rocks of Chapada consist of an expressive variety of gneisses, schists and quartzites that can

be grouped into five rock associations (Tab. 1 and Fig. 4; see also Kuyumjian et al. 2010).

Moore et al. (2019) in turn emphasize the occurrence of hydrothermal alteration at Chapada in the form of muscovite-chlorite, argillic, sericitic and potassic zones, interspersed with intermediate metavolcanic, metavolcanic-sedimentary and amphibolitic units. The deposit is centered on the potassic

alteration zone. A bed of manganiferous metachert (gondite) is mapped 6 km southeast of the deposit.

The Chapada orebody lies roughly along the contact between a massive bank of quartz-amphibole schist to the northwest and the above-mentioned intermediate volcanic and metavolcanic-sedimentary units to the southeast (cf. Kuyumjian 1989a). The deposit stratigraphy consists from

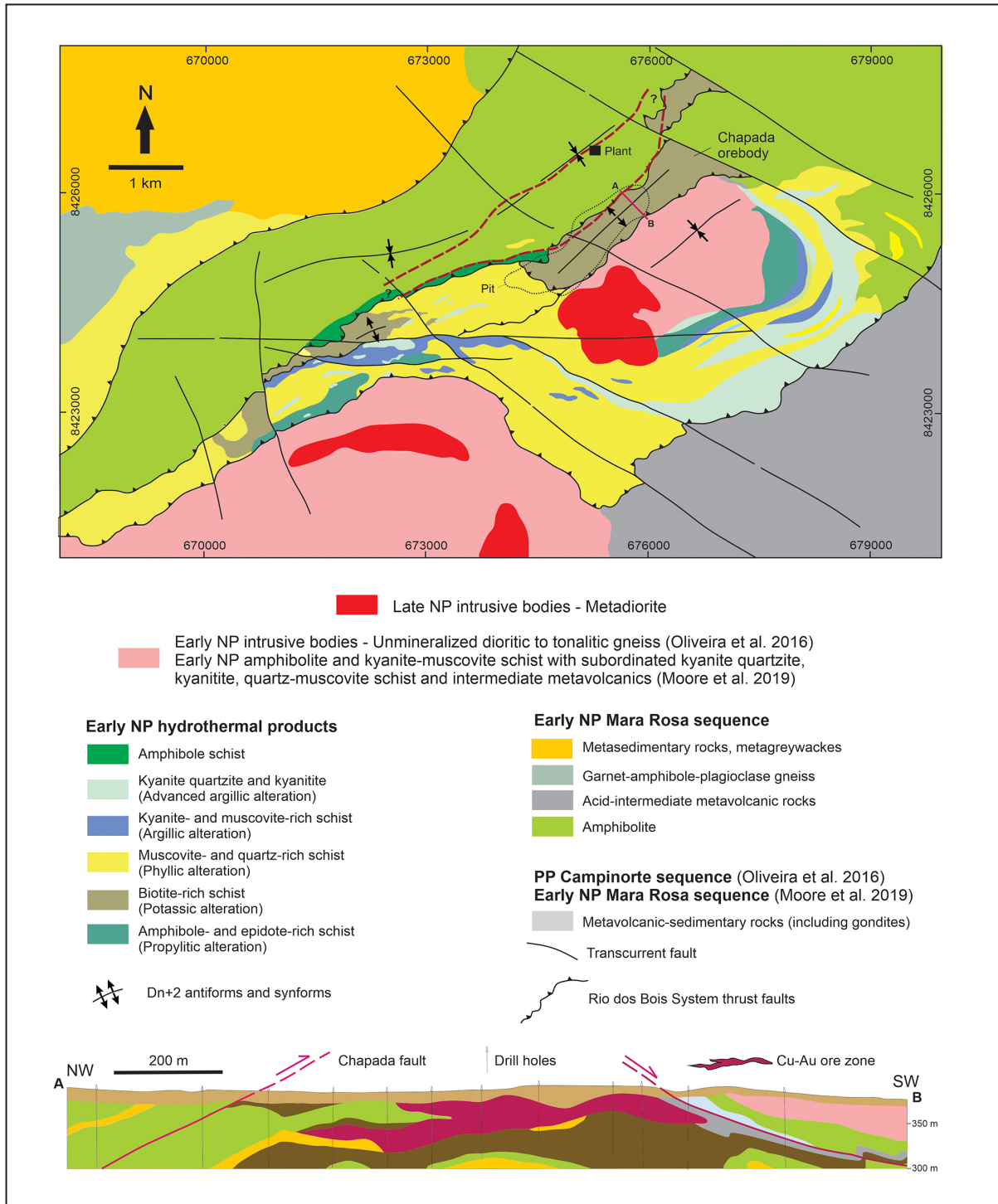


FIGURE 4. Geologic map of the Chapada deposit environs showing lithologic units, major structures, products of hydrothermal alteration, sectors of the orebody and pit contour. A cross-section (A-B) of the deposit is also shown (modified from Oliveira et al. 2016). Approximate location of epidote-rich amphibolite and epidosite shown by red traced line (from Kuyumjian 1989a, 1991, 1998a). PP, Paleoproterozoic and NP, Neoproterozoic. Note significant lithological differences between maps of figures 3 and 4, e.g., amphibolite areas in the former versus dioritic to tonalitic gneiss or volcanic-sedimentary rocks and alteration products in the latter. Note also differences with the map by Moore et al. (2019) referred to in the legend of this figure.

top to bottom of an upper sedimentary unit, the A, B and C intermediate volcanic rock-bearing 'layers', and a basal mafic volcanic-sedimentary unit. Plutonic dioritic and quartzdioritic porphyry gneisses occur associated with the supracrustal rocks, particularly with the main ore-hosting, the B Layer.

Characteristics of these rock units are presented in Table 2. Ore is hosted mainly in intermediate metavolcanic rocks of Layer B, and less so in similar rocks of Layer A. The volcanic protolith has been defined on basis of litho-geochemistry and petrography. Coincidentally, Layer B is the one which carries the highest proportion of intrusive orthogneissic

intercalations, which are ascribed as responsible for bringing in the mineralizing fluids, though, peculiarly, these gneisses themselves lack mineralization.

As to deformation and metamorphism of the Chapada deposit, Oliveira (2009) and Oliveira et al. (2016) recognize an early D_n isoclinal deformation episode that generated metamorphism of amphibolite-facies and a D_{n+1} shearing transpressional event in greenschist facies, besides a lesser D_{n+2} phase with open folding and brittle faulting. Moura et al. (2015), in turn, dated rutile of muscovite-quartz-kyanite schist of the deposit also via the U-Pb method and obtained an age

TABLE 1. Ore host rock associations of the Chapada deposit (compiled from Oliveira et al. 2016).

HOST ROCK ASSOCIATION	MAIN ROCK TYPES	OBSERVATIONS	MINERALIZATION
Amphibole- and epidote-rich rocks	Epidote-amphibole schist, epidosite, amphibolite, epidote amphibolite and epidote gneiss	Massive to finely foliated / Propylitic alteration	Rocks occasionally rich in pyrite and chalcopyrite mainly in epidote-amphibole schist
Biotite-rich rocks	Biotite-rich schists and gneisses Complex petrographic association of biotite schist, muscovite-biotite schist, amphibole-biotite schist and biotite gneiss. Mica layers can host porphyroblastic amphibole, kyanite, staurolite, garnet, feldspar, epidote, rutile and anhydrite	Potassic alteration superimposed mainly on equigranular metadiorite / porphyritic metadiorite and subordinately on metavolcanic-sedimentary rocks.	Most important host rocks of the deposit / Deformed chalcopyrite, pyrite and magnetite grains preferentially associated with biotite-rich domains
Muscovite- and quartz-rich schists	Schist made up mainly of muscovite, quartz, epidote, including banded chlorite-quartz-muscovite schist	Well-developed schistosity / Phyllic alteration / Association occurs in a wide area surrounding the deposit	Subordinate ore host rocks / Pyrite dominant sulfide, rutile and chalcopyrite common
Kyanite- and muscovite-rich schists / Quartzites and kyanitites	Quartz-kyanite-muscovite schist / Orthoquartzite, kyanite quartzite, quartz-kyanite rock, kyanitite	Argillic (schist) advanced argillic (quartz kyanitite) alteration / Access-ory phases include feldspar, epidote, staurolite, rutile, lazulite, anhydrite, roscoelite, tourmaline and corundum	Commonly pyrite-rich, chalcopyrite-poor and locally gold-bearing / Association occurs outside of the deposit

TABLE 2. Rock units and main rock types of the Chapada deposit (compiled from Moore et al. 2019).

ROCK UNIT	MAIN ROCK TYPES AND CHARACTERISTICS	PROTOLITHS (from petrography and litho-geochemistry)	MINERALIZATION
Metasedimentary layer	Garnet-biotite schist with small compositional variations, containing muscovite, staurolite, epidote and amphibole with disseminated pyrrhotite and pyrite	Large amounts of quartz (30%) suggest sedimentary protoliths	Disseminated pyrrhotite with subordinate pyrite and no economic mineralization
Upper Metavolcanic-Sedimentary Layer (A Layer)	Garnet-biotite-quartz schist as above / Epidote-garnet-staurolite-gedrite-hornblende-quartz schist / Epidote-muscovite-amphibole-biotite gneiss / Mylonitic biotite schist with porphyroclastic quartz-feldspar aggregates immersed in a sulfidic sericitized matrix	Sedimentary rock / Impure sedimentary rock of intra-arc igneous provenance / Intermediate volcanic rock / Tuffaceous rock, composition not referred to	Intermediate metavolcanic rocks of A Layer host the mineralization in the SW sector of Chapada
Metavolcanic Layer (B Layer)	Biotite-quartz schist, (amphibole)-biotite gneiss as A Layer / Abundant porphyry quartzdioritic & dioritic gneiss bodies / Intermediate metaplutonic porphyry bodies / Rocks of hydrothermal alteration haloes similar to figure 4	Sedimentary and intermediate volcanic rocks / Island arc M-type granitoids, early- & inter-late-mineral stocks / Late-mineral porphyry stocks / Potassic, sericitic, advanced argillic and propylitic alteration	Intermediate metavolcanic rocks are the most important ore host rocks of Chapada and B Layer contains the majority of the resources, but granitoid gneisses are not mineralized
Lower Metavolcanic-Sedimentary Layer (C Layer)	Metavolcanic-sedimentary rocks identical to A Layer.	Protoliths identical to A Layer	No mineralization
Mafic Metavolcanic-Sedimentary Layer	Fine-grained amphibolite interlayered with metasedimentary rocks	Basalts and sedimentary rocks	No mineralization

of 750 Ma, interpreted as the age of the upper amphibolite facies metamorphism over the argillic alteration zone of the deposit (cf. Fig. 4). The deformational and metamorphic picture for Chapada agrees with that reported in Junges et al. (2002, 2003), being related to collisional events of the Mara Rosa Arc tectonic history, as mentioned above. Further information on the Chapada deposit relevant to the present argument is disclosed in the following sections.

4 Litho-tectonic setting

Volcanogenic deposits have been classified on the basis of their host lithologies following a scheme that considers all strata within the host succession defining a distinctive deposit-related time-stratigraphic event (Barrie and Hannington 1999; Franklin et al. 2005; Galley et al. 2007). According to this approach, five 'lithologic types' have been recognized, viz., back-arc mafic, bimodal-mafic, pelitic-mafic, bimodal-felsic and felsic-siliciclastic, to the latter being added a hybrid VMS-epithermal subtype by Dubé et al. (2007). In general terms, these types correspond to different submarine tectonic settings, with the above-presented order reflecting the transition or change from the most primitive VMS environments, represented by ophiolite settings, through oceanic arc, evolved rifted arcs, continental back-arc to sedimented back-arc (e.g., Galley et al. 2007).

By virtue of its oceanic arc setting, mafic dominated lithological package and tectonic setting (cf. Richardson et al. 1986; Kuyumjian 1989a, b, 1991; Pimentel et al. 2000, 2004), the Chapada environment can be equated quite straightforwardly - almost by exclusion of the other types - with that of the bimodal-mafic type. This type features incipiently-rifted bimodal volcanic arcs above intra-oceanic subduction zones of collisional settings, i.e., an oceanic supra-subduction rifted arc in which basalt is dominant but up to 25% felsic volcanic strata may occur. Rock types consist predominantly of pillowed and massive basaltic flows, felsic flows, with subordinate felsic and mafic volcanoclastic rocks. These are accompanied by terrigenous sedimentary rocks mainly in the form of immature wacke, sandstone and argillite with local debris flows.

Practically all these attributes are represented in the general geology of Chapada, as shown in the previous and coming sections. Viana et al. (1995), for instance, report that orthogneisses of the Mara Rosa region - which are petrographically and geochemically comparable to those of Chapada 40 km to the SE - exhibit chemistry similar to M-type granitoids of immature island arcs. Kuyumjian (1989a, 1991) refers to the occurrence in the Chapada area of calc-alkaline metabasalts characteristic of arc and back-arc settings. The latter implies an extensional episode that is essential to the generation of exhalative deposits in the course of the predominantly compressive arc evolution. These metabasalts with associated metagabbros, and the metadioritic-tonalitic plus dacitic-rhyolitic gneisses compose the bimodal magmatism that also characterizes a transient extensional episode within an otherwise essentially collisional regime as already referred to. The above-mentioned sedimentary rock types are also represented in the Chapada - Mara Rosa region, i.e., metagreywackes, metasandstone and metargillites (e.g., Pimentel et al. 2000; Oliveira et al. 2016). In conclusion, it can be ascertained that Chapada fits the volcanogenic model in terms of its litho-tectonic setting.

5 The volcanogenic model and Chapada

5.1 Magmatic heat sources

A magmatic heat source has been considered one of the most important requirements for the occurrence of volcanogenic deposits, being usually represented by tholeiitic to low-K calc-alkaline shallowly emplaced quartz-diorite-tonalite-trondhjemite composite intrusive complexes (Galley 2002, 2003). They are co-magmatic with the volcanic rocks and can contribute metals to the hydrothermal system. In rifted oceanic arc settings, in particular, the anhydrous nature of bimodal magmas and the thinness of the crust result in the emplacement of the mentioned quartz-diorite-tonalite-trondhjemite complexes within 2 to 3 km from the sea floor and coeval with the VMS-hosting volcanic beds (Franklin et al. 2005). The volcanic-associated intrusive igneous bodies would point to vigorous long-lived convective hydrothermal systems adequate for the generation of sizable volcanogenic deposits. In some cases, layered mafic intrusions may also be involved. Still according to the above authors, high-temperature felsic and mafic rocks such as high-silica rhyolites and boninites are important indicators of high heat-flow environment conducive to generation of volcanogenic deposits. Palermo (1996b), for instance, suggests that part of the amphibolites in the Mara Rosa Arc may correspond to komatiites or boninites, a feature that points to a high-heat flow and, consequently, to potential generation of volcanogenic deposits.

Dioritic to tonalitic orthogneisses (cf. Fig. 4) associated with the Mara Rosa volcanic-sedimentary sequence could provide heat sources for a robust volcanogenic system at Chapada. To fit the model, however, age relationships between intrusive and supracrustal rocks should overlap. Regarding this, according to Kuyumjian (1989b, 1991, 1995), metagabbros and gneisses of Chapada are coeval with metabasalt and felsic metavolcanic rocks, and the magmatism during generation of the deposit was mainly intrusive, represented principally by diorite-tonalite plutons that were co-magmatic with the evolution of the Mara Rosa sequence. In support of this, the author refers to U-Pb zircon ages of 862 ± 8 Ma and $856 \pm 13/-7$ Ma obtained, respectively, from felsic metavolcanic rock and metatonalite of the Mara Rosa region (Posse deposit) by Pimentel et al. (1993) and Viana et al. (1995), and considered by these authors as indicative of the generation age of their respective protoliths. However, the above-mentioned felsic metavolcanic rocks of the Posse mine ('felsites') were reinterpreted as mylonitized granite by Palermo et al. (2000) on grounds of the presence of sparse coarse-grained texture and antiperthite. Oliveira (2009) reassures the late emplacement of the diorite-tonalite plutons for the Chapada deposit area itself. According to this author, U/Pb zircon data revealed ages of 884.9 ± 9.4 Ma and 864.9 ± 5.6 Ma for a feldspathic biotite schist and a biotite gneiss, respectively. The results are interpreted as the ages of the related protoliths, namely, a volcanic rock considered as the protolith of Mara Rosa felsic metavolcanic rocks and an acid to intermediate plutonic rock, typical of volcanic arc environment.

Oliveira et al. (2016) present additional U-Pb zircon age data results for rocks of Chapada, viz., 930-890 Ma (mean 908 Ma) for an ore-hosting volcanoclastic feldspathic muscovite schist, 867 ± 8 Ma for an equigranular magnetite-biotite metadioritic gneiss, 884 ± 15 Ma for a porphyritic metadioritic gneiss and 634.8 ± 6.8 Ma for a younger, weakly

deformed metadiorite. Zircon crystals are reportedly pristine and hence record crystallization ages in the case of igneous protoliths and the age of volcanic activity in the case of the volcanoclastic schist.

More recently, U-Pb dating presented by Moore et al. (2019) revealed an age of 908 Ma for a fine-grained mylonitic biotite-schist metatuff of Chapada. The result, according to the same source, indicates the timing of volcanic activity in the Mara Rosa Arc. Additionally, an early-mineral meta-quartzdiorite porphyry and a late-mineral metamorphosed intermediate porphyry intrusive rock of the deposit yielded U-Pb ages in zircon of 884 ± 5 Ma and 879 ± 5 Ma, respectively. It is possible, however, that the age result on the metatuff is the same as that of Oliveira et al. (2016).

The above information is summarized in Table 3. To sum up the subject, robust U-Pb data shown indicate that the age relationships between Mara Rosa supracrustals and associated intrusive rocks at Chapada vary from a gap of ca. 25 Ma (908 to 884, respectively) to a possibly negligible age difference (minimum 885 ± 9 Ma for volcanic rocks and maximum 884 ± 15 Ma for plutonic gneisses), whereas at Posse the two ages practically overlap. Therefore, it can be concluded that the ages of the Mara Rosa volcanic-sedimentary rocks and associated intrusive gneissic stocks overlap to a certain extent. This notwithstanding, it is relevant to note that the most voluminous phases of VMS-related subvolcanic intrusions can actually be emplaced later than the mafic and felsic volcanic rocks directly hosting, or associated with, the volcanogenic deposits (cf. Galley 2002, 2003), so that a strict age-match between volcanic-sedimentary units and related intrusive bodies is not universal in volcanogenic systems.

5.2 Regional semi-conformable alteration zone

Semi-conformable alteration zones occur stratigraphically below the orebodies and have been considered the source sites of metals and sulfur of volcanogenic hydrothermal systems, e.g., Franklin (1996), Galley (1993), Santaguida et al. (2002), Franklin et al. (1981, 2005) and Galley et al. (2007). The semi-conformable alteration systems consist of vertically stacked zones that superficially resemble regional metamorphic facies. The individual zones include chloritization, spilitization, silicification and epidotization. They are controlled in extent

by the strike and length of an underlying intrusion, and are generally horizontal and stratified, developing in conformity with the isotherms above the cooling intrusion. The stratified alteration zones as a whole can have a strike length of 5 to 50 km and a thickness of 1 to 3 km. The size and areal morphology of VMS deposit clusters reflect those of the underlying semi-conformable alteration zone (Galley 1993; Galley et al. 2007). According to Franklin (1996 and references therein), these zones occur several hundreds of meters or more below the massive sulfide deposits, and may represent part of the 'reservoir zone' wherefrom the metals and sulfur were leached prior to their ascent to and expulsion onto the sea floor. The semi-conformable regional alteration zone may include in its middle portion an impermeable barrier in the form of a confining bed or cap rock, such as a silicified zone. This barrier restricts and insulates the lowermost zone of the hydrothermal system, allowing for a more efficient metal leaching, and is periodically breached, e.g., by seismic activity, allowing focused upflow of metal-rich fluids to the seafloor via synvolcanic faults to generate volcanogenic deposits (Franklin et al. 2005; Galley et al. 2007). Franklin (1993, p. 328), citing Hodgson and Lydon (1977), considers this impermeable cap to the hydrothermal reaction zone as the most important factor in the formation of massive sulfide deposits.

These large alteration zones have been recognized below deposits in several massive sulfide districts of Canada, e.g., Noranda, Mattagami and Snow Lake. They consist in their deeper section mainly of laterally extensive quartz-epidote zones that are several hundred meters thick, extending downwards to a few hundred meters stratigraphically below the deposits. Santaguida et al. (2002) consider that such zones of strong alteration contain >15% epidote and affect with particular intensity mafic rocks in the vicinities of volcanic centers. They have been related to an increase in heat flow resulting from convective heat transfer away from cooling intrusions at the base of the hydrothermal systems. They represent a zone of high temperature hydrothermal reaction (ca. 400°C), under low water-rock ratio conditions, where the metals and sulfur entered into the ore-forming solution. Therefore, all of these epidote-quartz zones are metal depleted (cf. Franklin 1996). Losses of as much as 90% of their original copper content and 70% of their zinc are referred to by Franklin et al. (2005).

TABLE 3. Summary of U-Pb zircon age data of the Mara Rosa - Chapada arc sector.

AGE	ROCK TYPE	LOCATION	GEOLOGY / PROTOLITH	REFERENCES
807 ± 5 Ma	Tonalitic orthogneiss	25 km SE of Mara Rosa	Arc intrusive complex	Junges et al. (2003)
862 ± 8 Ma	Mylonitic granite (ex-felsic metavolcanic rock)	Posse (Au-only)	Mara Rosa mineralized sequence	Viana et al. (1995), Palermo et al. (2000)
856 +13/-7 Ma	Tonalitic gneiss	Posse (Au-only)	Arc intrusive complex	Pimentel et al. (1993), Viana et al. (1995)
884.9 ± 9.4 Ma	Kyanite-epidote-muscovite-biotite feldspathic schist	Chapada (Cu-Au)	Volcanic rock of ore host sequence	Oliveira (2009)
864.9 ± 5.6 Ma	Magnetite-biotite gneiss	Chapada (Cu-Au)	Acid to intermediate plutonic rock	Oliveira (2009)
908 Ma (mean)*	Feldspar-kyanite-epidote-muscovite-biotite schist**	Chapada (Cu-Au)	Volcanoclastic rock of ore host sequence	Oliveira et al. (2016)
867 ± 8 Ma	Magnetite-biotite gneiss	Chapada (Cu-Au)	Equigranular diorite; pristine zircon	Oliveira et al. (2016)
884 ± 15 Ma	Porphyritic gneiss	Chapada (Cu-Au)	Porphyritic diorite; pristine zircon	Oliveira et al. (2016)
634.8 ± 6.8 Ma	Younger metadiorite	Chapada (Cu-Au)	Slightly deformed diorite	Oliveira et al. (2016)
908 Ma	Sulfidic, sericitized mylonitic biotite schist**	Chapada (Cu-Au)	Metatuff, ore-host supracrustal sequence	Moore et al. (2019)
884 ± 5 Ma	Intermediate metaquartz-dioritic porphyry gneiss	Chapada (Cu-Au)	Early-mineral intrusive stock	Moore et al. (2019)
879 ± 5 Ma	Intermediate porphyry metaplutonic intrusive	Chapada (Cu-Au)	Late-mineral intrusive stock	Moore et al. (2019)

*(930-890 Ma) (**Same rock type, same analysis?)

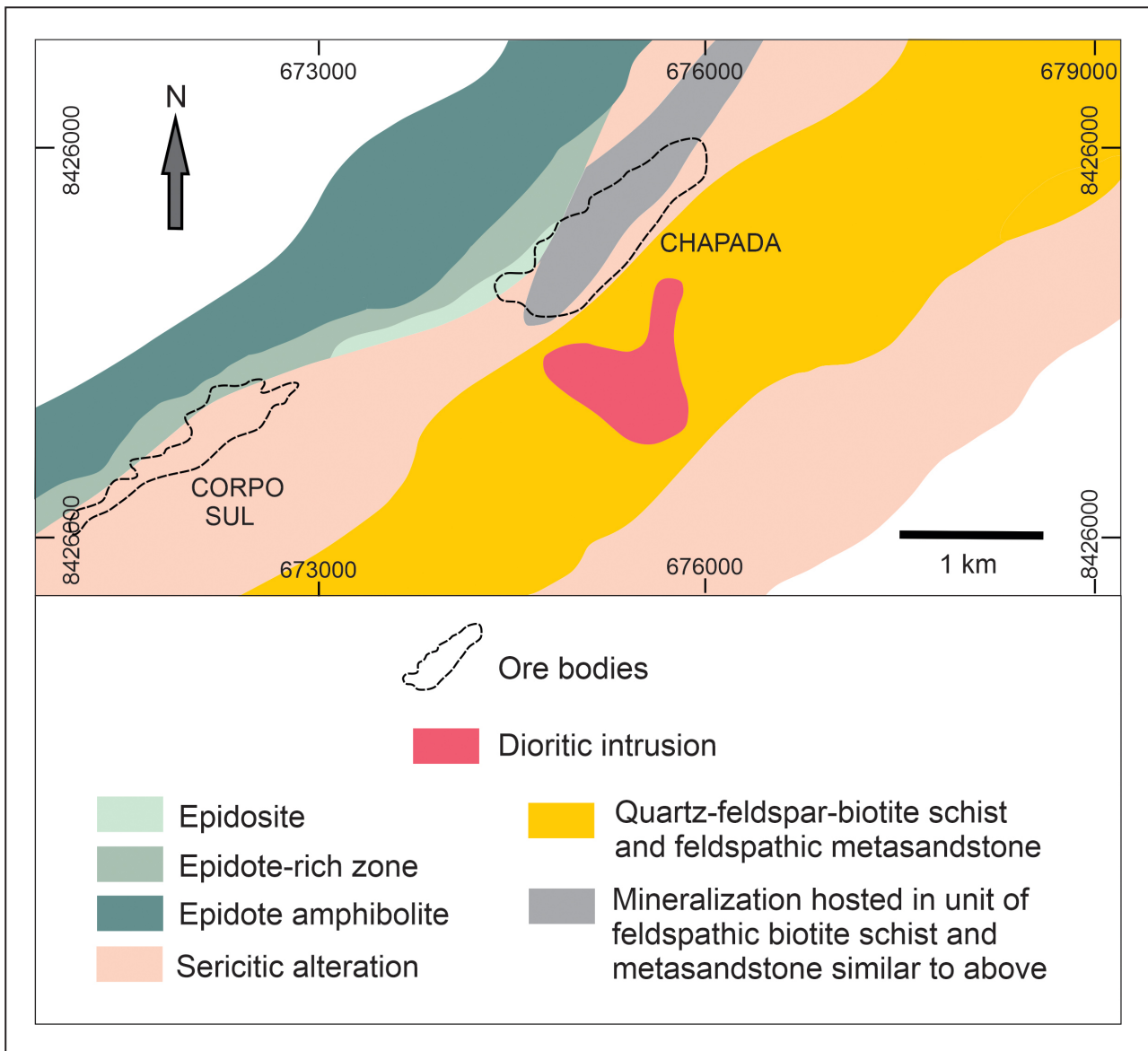


FIGURE 5. Simplified geology of the Chapada deposit environs showing the distribution of the epidote amphibolite, epidote-rich and epidosite zones west and northwest of the mineralized area (from Kuyumjian 1989a, 1998a). Location of orebodies is approximate (from Oliveira et al. 2016, cf. Figure 4). Note the geologic differences between this map and those of figures 3, 4, and 13, reflecting different authors and/or different stages of the mapping of the area.

In the case of Chapada, Kuyumjian (1989a, 1991, 1995, 1998a, 2000) describes regional epidote-rich alteration in the form of a widespread zone of epidote-rich amphibolites and epidosites, about 0.5-1 kilometer-wide, lying immediately west and north of the deposit and extending to NE and SW for at least 5 km (Figs. 3, 4, 5 and 6). These rocks are inserted in a regional unit of epidotized amphibolites, which extends for at least 50 km (Kuyumjian 1989a).

The epidote-rich amphibolites of Chapada commonly carry up to 60% of modal epidote and contain narrow bands of epidosite, a striped rock composed of epidote, quartz, sphene and subordinated magnetite, with variations containing almost only epidote and sphene. This epidote-rich basalt zone of Chapada is reminiscent of the above-described type of regional volcanogenic alteration zone so much so that Kuyumjian (1989a, 1991, 1998a) considers that it represents the afore-mentioned reaction or reservoir source zone of hydrothermal fluids that up-flowed via synvolcanic



FIGURE 6. Deformed epidote-rich amphibolite of Chapada, showing stretched and boudinaged bands of epidote (from Kuyumjian 1989a). Rock contains commonly up to 60% of this mineral.

conduit faults to generate volcanogenic (pre-metamorphic) mineralization. For Kuyumjian (1989a), based on Richardson et al. (1987), these epidote-rich rocks are very similar to hydrothermal epidiosites of the Troodos Complex of Cyprus, which contain well-known copper-bearing volcanogenic massive sulfide deposits. Kuyumjian (1989a) also notes that the epidiosite forms a several meter-thick layer that runs for several kilometers just west of the Chapada deposit. It is suggested here that this kind of horizon or blanket may have acted as a confining cap rock bed that catalyzed the metal-stripping power of the underlying epidotization zone (cf. Franklin 1996, p. 177; Franklin et al. 2005, p. 540, and Figure 14 in section 6). Alternatively, the striped epidiosite may represent an exhalite, as discussed in section 5.6.

Kuyumjian (1989a) also notes that some amphibolites located west of the Chapada deposit show enrichment in Na_2O and depletion of K_2O and that this chemistry could point to spilittization of the basaltic precursors of the amphibolites.

The position of the epidote-rich amphibolites and spilittized metabasalts west and north of the Chapada deposit suggests, if not indicates, a stratigraphic situation of general southeastwards facing.

5.3 Synvolcanic faults

Synvolcanic faults control the location and discharge of hydrothermal fluids by allowing the access from the underlying reservoir alteration zones. They may be represented, for instance, by main listric, rifting-related faults, of either axial- or boundary-rift position, that may have been overprinted and reactivated as wrench or thrust faults (Large 1992; Huston 2000). Transgressive silicified and intense phyllic alteration zones, vein and disseminated sulfides, synvolcanic dykes and dyke swarms, and deposit-limiting faults may all indicate the location of synvolcanic faults (e.g., Large 1992; Franklin 1996, Franklin et al. 2005). The incidence of alteration along fault zones or narrow vertical zones in a volcanic environment has also been interpreted as indication of the synvolcanic nature of faults (Franklin et al. 2005). Deformation and metamorphism of course may pose difficulty on the recognition of the original location, nature and role of these structures.

Regarding the Chapada deposit, various authors have proposed or described possible indications of structural controls on the setting of the deposit and the generation of ore itself, with particular reference to the role of the Rio dos Bois shear zone and ancillary faults (e.g., Kuyumjian 1995; Ramos Filho et al. 2003, 2005; Oliveira 2009, Oliveira et al. 2016).

For the present exercise, however, it is important to emphasize the aspect that early, basin-related faults acted as synvolcanic hydrothermal conduits. Reference to this aspect is missing in the literature of Chapada, given the natural difficulties of definition of the original structural framework of the basin in this highly metamorphosed and deformed terrain. Perhaps the only exception to this is the suggestion by Kuyumjian (1989a) that faults related to the continental-scale Transbrasiliiano lineament (Fig. 2) may have channeled the volcanogenic hydrothermal fluids of the deposit. As another possibility, this role might have been played by precursors of the Rio dos Bois fault system. Some of these precursors might have evolved, for instance, into the amphibolite facies D_n and greenschist facies D_{n+1} shear and thrust zones that have been interpreted as important structural controls of Chapada by the above-mentioned authors.

With this structural picture in mind, one may speculate that the fault systems presently recognized at Chapada and environs may have in part overprinted previous zones of weakness from an early rift-stage fault framework that originally controlled synvolcanic fluid discharge in the Mara Rosa Arc basin and were reactivated during the deformational development of the fold belt. The possible conduit role or synvolcanic nature of these faults is reinforced by features such as more intense alteration occurring along regional fault zones (Kuyumjian 1995), deposit control by $\text{N}20^\circ\text{E}$ -trending shear zones (Kuyumjian 1998a), and the deposit abutting a 40 m wide, NE-trending, shallow-dipping, mylonitic thrust fault that is part of the Rio dos Bois system (Richardson et al. 1986) (Fig. 7). According to these last authors, the mylonitic zone bounds the deposit on its south side and separates it from a porphyritic diorite intrusion showing tight isoclinal to broadly open folds (3-5 m wavelength). This kind of orebody-limiting fault is usual in exhalative deposits, as exemplified in Goodfellow et al. (1993, p. 234-237) and Franklin (1993, p. 329).

Another interesting piece of speculation in connection with this subject is the suggestion made by Oliveira et al. (2016, p. 17) about the regional linear distribution of aluminous alteration in the Chapada region. According to these authors, this pattern may have resulted from longitudinal faults coeval with the arc development that controlled the distribution of dyke-like bodies of porphyry rocks, which constituted the protoliths of the altered rocks. The potential role of this kind of faults as synvolcanic hydrothermal conduits does not need to be emphasized here.

5.4 Deposit-scale alteration products

Deposit-scale hydrothermal alteration has been the most extensively studied aspect of volcanogenic deposits and even a brief description of this feature involves significant detail. Alteration is commonly concentrated in the footwall and, according to Galley et al. (2007), in greenschist facies systems it usually consists of (cf. Fig. 8):

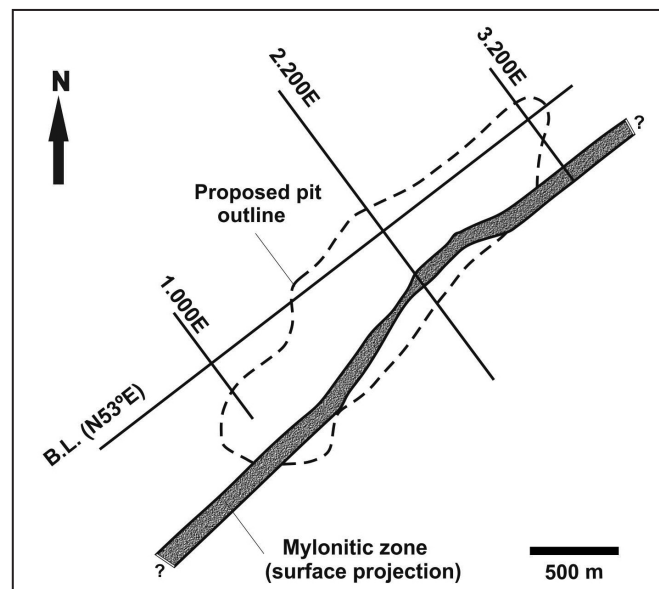


FIGURE 7. Sketch showing the originally proposed pit outline of the Chapada mine and the surface projection of the deposit southeast-limiting mylonitic zone (from Richardson et al. 1986).

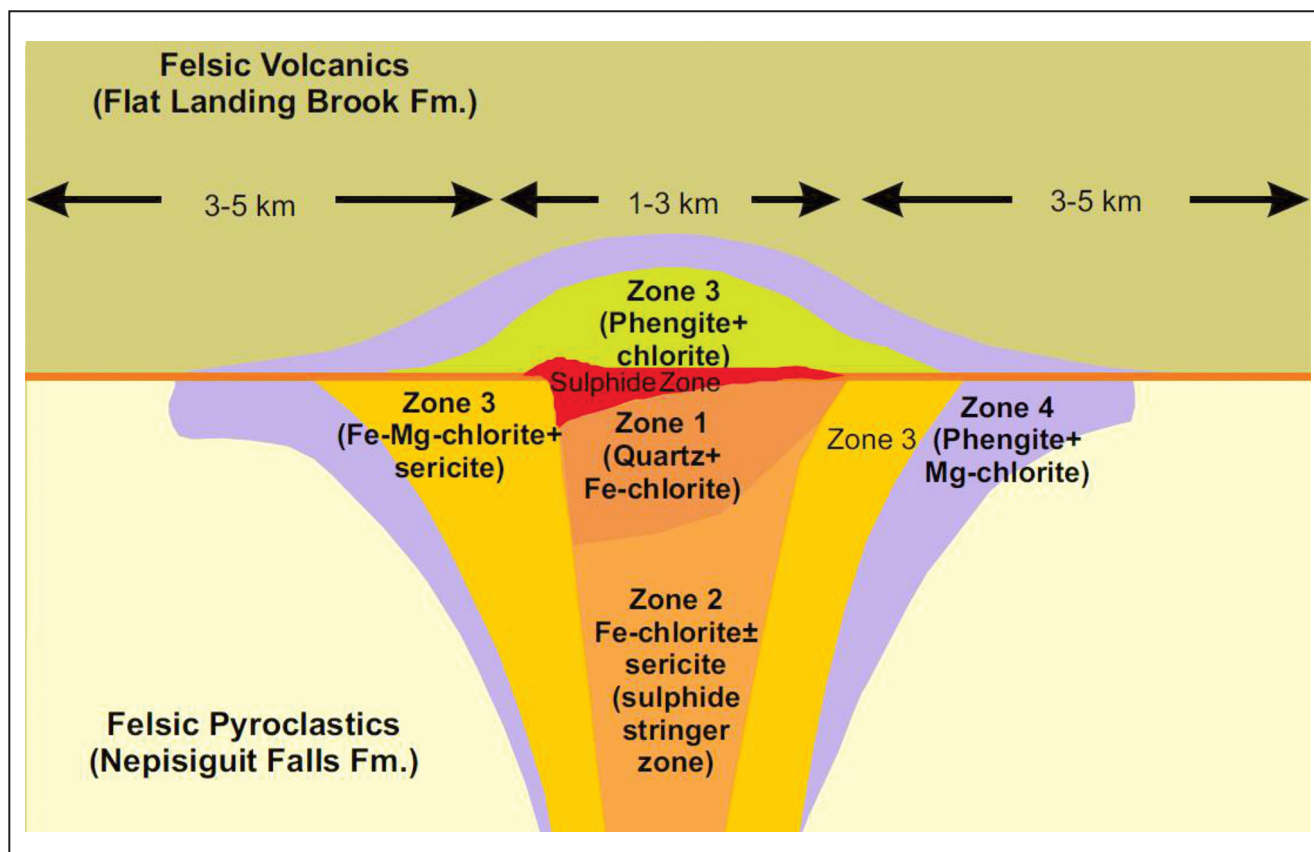


FIGURE 8. A schematic composite section through a VMS alteration system in the Bathurst mining camp as an example of VMS proximal alteration zone metamorphosed to greenschist-facies mineral assemblages (from Goodfellow et al. 2003, in Galley et al. 2007).

- A Fe-chlorite-quartz-sulfide \pm sericite mineral assemblage, which is commonly associated with the core of stockwork vein mineralization, or stringer ore, and becomes increasingly quartz- and sulfide-rich towards the lower contact of the massive sulfide lens. In some cases, talc and/or magnetite occur at the top of this alteration pipe.

- The core is enveloped by a wider zone of Fe-Mg-chlorite-sericite, including phengite (high-silica muscovite) in the part of this zone that encompasses the immediate hanging wall to the massive sulfide lens. Outboard from this is a fringe rich in sericite, phengite and Mg-chlorite \pm albite \pm carbonate \pm barite. This outer alteration zone may also include a portion of the hanging wall strata above, and lateral to, the massive sulfide lens.

Specifically, for the case of basalt-dominated settings of the bi-modal mafic type of oceanic arcs – a situation that applies to the Chapada deposit (cf. section 4) - Franklin et al. (2005) describe a well-defined pipe with width to depth ratio of \sim 1:10 that may extend for paleodepths of hundreds of meters. It consists of a Fe-chlorite + pyrrhotite-chalcopyrite core and a Mg-chlorite + sericite + pyrite-sphalerite marginal zone, accompanied by local zones of silicification and in many cases pods of massive talc \pm magnetite \pm Mg-biotite.

For Precambrian deposits formed in shallow waters (cf. Mattabi-type; Morton and Franklin 1987; Franklin 1996), underlying pipes are silicified as well as sericitized, and aluminosilicate minerals are abundant. At the Chisel Lake deposit of the Snow Lake camp, Manitoba, for instance, a sericite-kyanite zone parallel to the paleosurface overlies a chlorite-staurolite zone that in turn is enveloped by a

biotite-garnet zone, the mineralogy reflecting amphibolite-facies metamorphism (Galley et al. 1993, in Galley et al. 2007; Fig. 9).

Galley et al. (2007) reinforce this picture by stating that in volcanogenic deposits of the shallow-water Mattabi-type, aluminosilicate minerals are actually prominent. Their high metamorphic grade equivalents include andalusite, anthophyllite, gedrite, cordierite and sillimanite. More aluminous assemblages commonly occur closer to a high-temperature alteration pipe.

For gold-rich volcanogenic deposits specifically, Dubé et al. (2007) indicate a pipe with central copper-gold stockwork / replacement ore giving place outwards to alumina-rich (advanced argillic) and clay-sericite (argillic) alteration zones, and upwards to a pyritic gold stockwork ore and a siliceous pipe. Besides this, there is a lower outer propylitic zone with Mg-chlorite and an upper outer carbonate \pm anhydrite zone (Fig. 10). Additionally, it should be noted that alumina-rich alteration may also be found in gold-poor deposits (Poulsen and Hannington 1996).

Regarding alteration and metamorphism, Bonnet and Corriveau (2006, 2007) and Shanks III (2012) synthesize the main mineralogy of alteration of volcanogenic deposits for pristine, greenschist and granulite facies conditions. These authors recognize five main types of VMS-related alteration types, viz., advanced argillic, argillic, sericitic, chloritic and carbonate propylitic, and present diagnostic minerals for each type in different metamorphic facies (Table 4). Mineralogical assemblages corresponding to the amphibolite facies were added on (from Dreher A.M., personal communication).

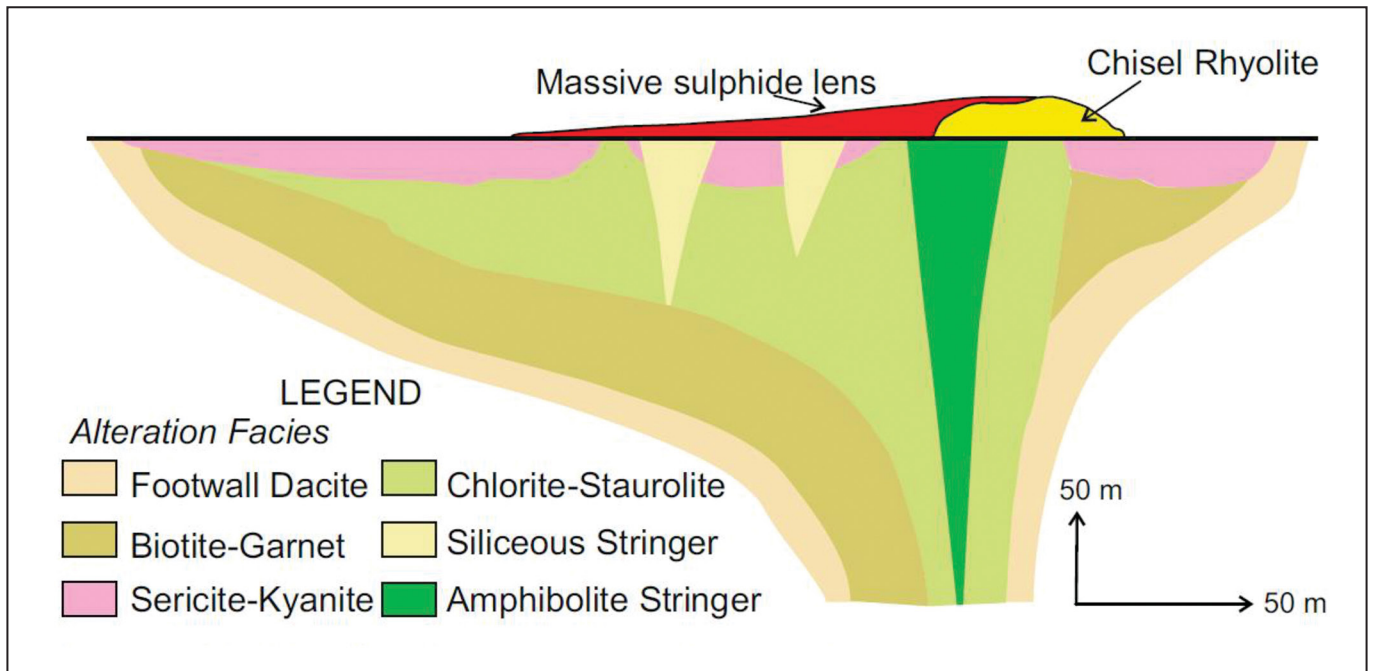


FIGURE 9. A stylized cross-section through the proximal alteration zone at the Chisel Lake deposit, Snow Lake mining camp, Canada, illustrating mineral assemblages of lower- to middle- amphibolite grade regional metamorphism (from Galley et al. 1993, in Galley et al. 2007).

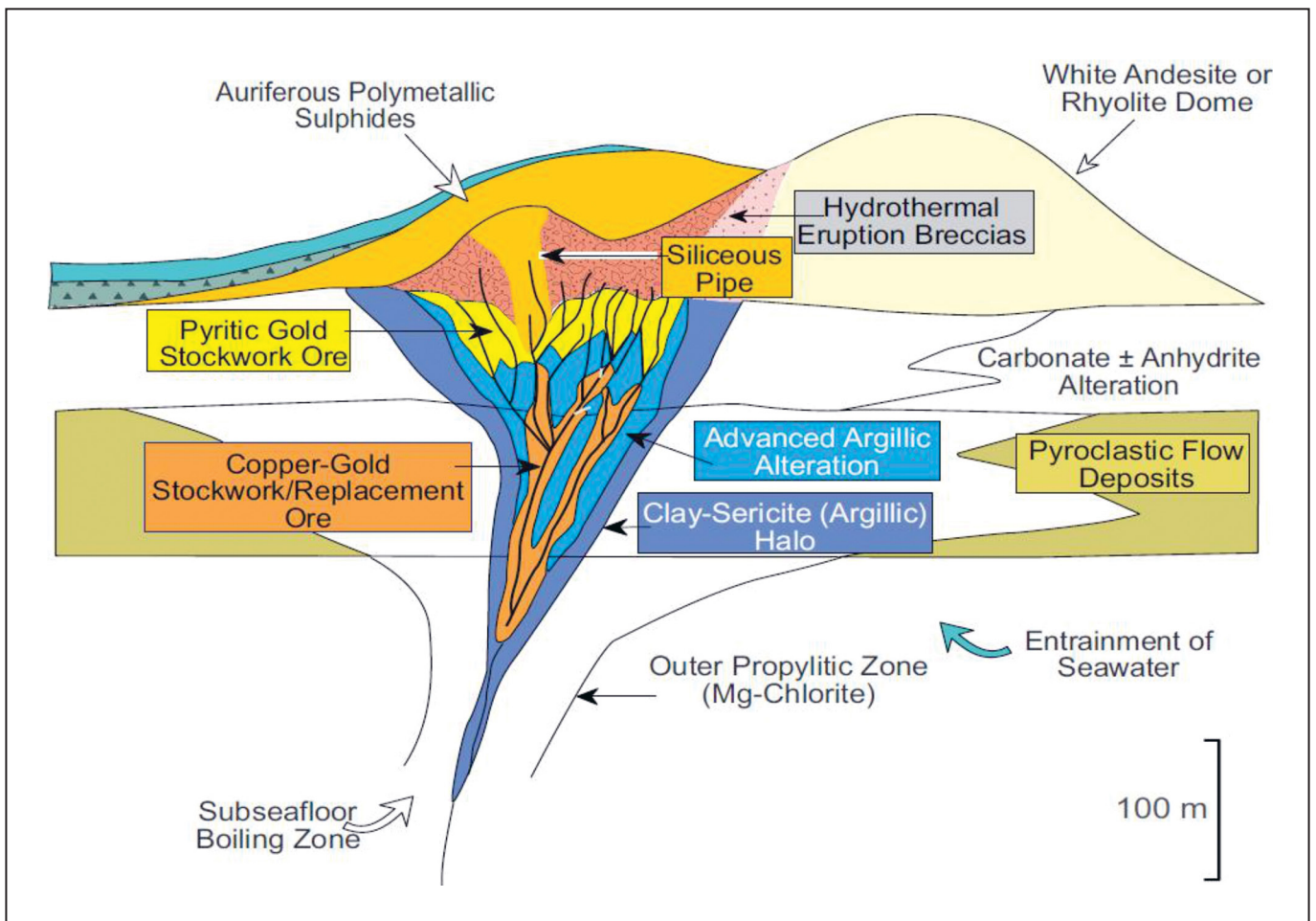


FIGURE 10. Schematic illustration of the geologic setting and hydrothermal alteration associated with Au-rich volcanogenic massive sulfide deposits. Note the incidence of argillic, advanced argillic, propylitic and carbonate ± anhydrite alteration haloes, besides pyritic-gold and copper-gold stockwork zones as well as a siliceous pipe (from Dubé et al. 2007, inspired in Hannington et al. 1999).

TABLE 4. Diagnostic hydrothermal alteration minerals of VMS deposits at different metamorphic facies (modified from Shanks III 2012 and Bonnet and Corriveau 2007 with addition of the amphibolite facies mineralogy according to Ana Maria Dreher, personal communication).

ALTERATION TYPE	DIAGNOSTIC MINERALS			
	NO METAMORPHISM	GREENSCHIST FACIES	AMPHIBOLITE FACIES	GRANULITE FACIES
Advanced argillic	Kaolinite, alunite, opal, smectite	Kaolinite, pyrophyllite, andalusite, corundum, topaz	Andalusite, sillimanite, kyanite, quartz, biotite	Sillimanite, kyanite, quartz
Argillic	Sericite, illite, smectite, opal, pyrophyllite	Sericite, illite, pyrophyllite	Muscovite, biotite, sillimanite, kyanite, garnet, cordierite	Sillimanite, kyanite, quartz, biotite, cordierite, garnet
Sericitic	Sericite, illite, opal	Sericite, illite, quartz	Biotite, K-feldspars, quartz, andalusite, sillimanite, kyanite	Biotite, K-feldspar, sillimanite, kyanite, quartz, cordierite, garnet
Chloritic	Chlorite, opal, quartz, sericite	Chlorite, quartz, sericite	Cordierite, phlogopite, K-feldspar, orthoamphibole (anthophyllite, gedrite), garnet, quartz, staurolite	Cordierite, sillimanite, kyanite, orthopyroxene, ortho-amphibole, phlogopite
Carbonate propylitic	Carbonate (Fe, Mg), epidote, chlorite, sericite, feldspar	Carbonate (Fe, Mg), epidote, chlorite, sericite, feldspar	Amphibole (actinolite, hornblende), Ca-plagioclase, epidote, quartz	Carbonate, grossular, epidote, hornblende, diopside, orthopyroxene

Additionally, anhydrite can also occur as an alteration or exhalation phase in volcanogenic systems. Galley et al. (2007, cf. Figure 1 therein, after Hannington et al. 1999), for instance, indicate the occurrence of anhydrite in the upper reaches of exhalative centers in the mid-Atlantic ridge, including anhydrite cones. Franklin (1993, p. 329) describes the deposition of anhydrite from rising hydrothermal fluids in seawater-filled cracks subjacent to Proterozoic or younger volcanogenic deposits, provided that the ambient seawater contained abundant dissolved sulfate, sealing the fluid conduits from the ingress of fresh seawater. Dubé et al. (2007) in turn show anhydrite associated with carbonate as a distal alteration product of gold-rich volcanogenic deposits. As a specific example, Franklin et al. (1981, p. 508) as well as Walford and Franklin (1982, p. 502) cite the occurrence of abundant anhydrite in the stringer zone of the Snow Lake massive sulfide deposits of Manitoba, Canada, where the gangue mineralogy includes quartz, cordierite, staurolite, and albite. Anhydrite occurs as well in some parts of the massive ores of the Snow Lake district.

In accordance with the picture on deposit-scale hydrothermal alteration detailed above, Chapada exhibits the following features that parallel those of the volcanogenic model, as indicated by Kuyumjian (1989a, 1991, 1995, 1998a,b, 2000) and Kuyumjian et al. (2010), as partly illustrated in Figure 11:

- Fe-Mg alteration indicated by rock types such as gedrite-anthophyllite-staurolite-enriched schists, some containing up to 70% gedrite, representing a chloritic alteration assemblage submitted to a high-amphibolite metamorphic rank; close association of the staurolite-gedrite-bearing rocks with the mineralized zones.

- Aluminous alteration in the form of kyanite and sillimanite-muscovite schists and quartzites (Fig. 3) that were originally interpreted as altered mafic lavas by Costa (1984, in Angeiras et al. 1988); and, locally, represented by peraluminous staurolite-kyanite amphibolite, also interpreted as derived from a basaltic protolith. The staurolite exhibits a lower content of SiO₂ and higher values of MgO, MnO and ZnO as compared to staurolite from adjacent metasedimentary rocks.

- Potassic phyllic (i.e., sericitic) alteration represented by pyritic magnetite-quartz-sericite schists that bound the ore zone, and potassium metasomatism suggested by the

presence of microcline and biotite in the ore-hosting schist along with a K₂O content as high as 7.13%.

Richardson et al. (1986) in turn mention that some amphibolites of Chapada exhibit possibly mixed Mg-Al alteration as indicated by their content of Mg-Al-enriched, moderately pyrope garnet (P_{y20} to P_{y25}). Besides this, Oliveira et al. (2016) report the occurrence of two opposed types of alteration at Chapada, namely, an upper zone of peraluminous kyanite- and muscovite-rich products and a lower, deeper one, of biotite-rich rocks with intervening muscovite- and quartz-rich rocks. These products are interpreted as advanced argillic (epithermal lithocap), potassic and phyllic / sericitic alteration, respectively. The presence of anhydrite veinlets is also referred to.

Finally an updated account of hydrothermal alteration at Chapada presented by Moore et al. (2019) indicates the following correlation between lithotypes and alteration halos occurring at the ore-hosting metavolcanic layer described by these authors:

- Biotite schist, muscovite-biotite schist, feldspathic-biotite schist, feldspathic muscovite-biotite schist, and quartz-biotite schist interpreted as the metamorphosed, ore-associated potassic halo. Anhydrite veinlets are commonly found in biotite-rich gneiss and schist.

- Biotite-muscovite-quartz schist and muscovite-quartz schist interpreted as a metamorphosed sericitic halo.

- Kyanite-muscovite-quartz schist, muscovite-kyanite-quartz schist, kyanite quartzite, muscovite quartzite, and kyanite interpreted as a metamorphosed advanced argillic halo.

- Epidote-rich rocks, e.g., epidosite and epidote-bearing schist with more than 20% epidote, interpreted as a metamorphosed calcic halo.

- Mostly unaltered wall rocks with sparse concordant epidote veins or with chloritized matrix interpreted as a metamorphosed propylitic halo.

These alteration products show a rough lateral zonation, as is somewhat evident from the above description confronted with Figure 4. The potassic alteration occurs in direct association with the deposit in the west, with sericitic or phyllic alteration lying eastwards and argillic, advanced argillic and propylitic alterations further east.

At this stage, it can be argued that the summary and examples presented in the initial part of this section are of significance regarding the present argument on the Chapada

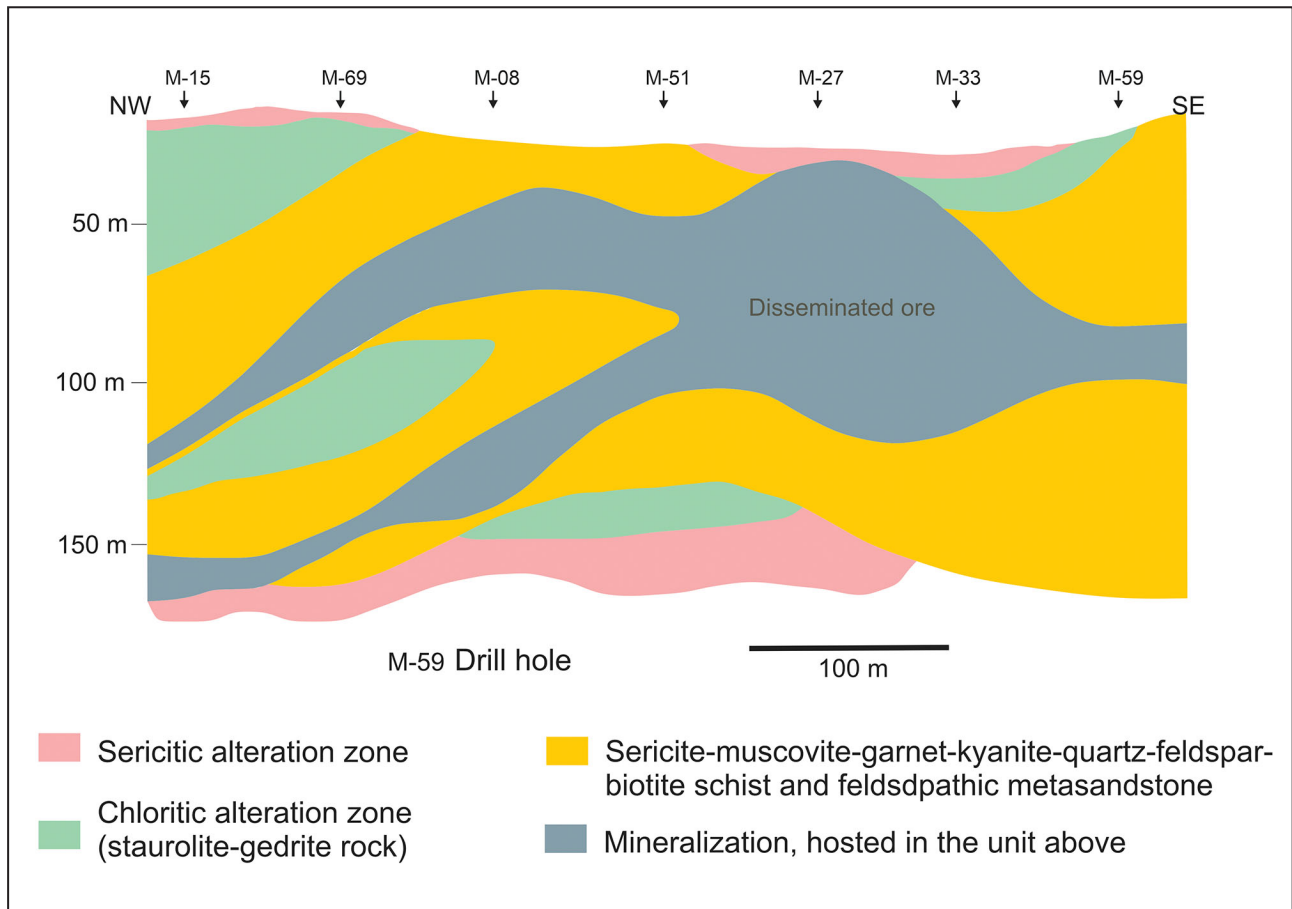


FIGURE 11. Geologic cross-section of the Chapada deposit (from Kuyumjian 1989a and Oliveira et al. 2004). Location of the section is shown in Figure 3.

deposit, as they exemplify the occurrence in the volcanogenic environment of various features of the deposit, including, for instance, the association magnetite-biotite-sulfides and the presence of zones of biotitic, sericitic, argillic, advanced argillic, and propylitic alteration (Fig. 4 and Tables 1, 2, and 4). To reinforce the argument, it should be stressed that all hydrothermal alteration zones known at Chapada have counterparts in volcanogenic systems. The same, perhaps, also holds roughly for the alteration zonation. Therefore, we defend that a significant parallel exists between Chapada and volcanogenic deposits in terms of proximal, deposit-scale hydrothermal alteration products. The relatively diversified alteration assemblages of Chapada may be ascribed to the prograde metamorphism to high-amphibolite facies and subsequent retrogression to greenschist facies.

Specifically, the occurrence of biotite as an important alteration product at Chapada can be explained from a volcanogenic standpoint by the incidence of medium-high grade metamorphism on rocks that had earlier undergone argillic, chloritic, or sericitic alteration (cf. Bonnet and Corriveau 2007 and Tab. 4). According to this source, chloritic alteration (Si+Al+Mg+Fe±K), which constitutes a kind of hallmark signature of many volcanogenic deposits, consists in low-grade metamorphic terrains of Fe-Mg-schist made up mainly of chlorite, quartz and sericite. This assemblage submitted to rising temperature (above 425 °C) turns into muscovite, phlogopite and quartz. In the case of sericitic alteration (Si+Al+K+Fe or Mg), primary products like sericite, quartz and sulfides are destabilized during prograde metamorphism to

form biotite, K-feldspar, aluminosilicate minerals and quartz at amphibolite and granulite facies. Paradis et al. (2002) also indicate the occurrence of biotite as an almost ubiquitous component of alteration zones in the core and margins of footwall alteration zones as well as in the hanging wall of several deposits of the Snow Lake district, Canada. As to anhydrite – also reported as an alteration product in Chapada (Richardson et al. 1986; Moore et al. 2019) – it should be mentioned that the mineral is equally found in volcanogenic systems, as indicated above, for instance, by Dubé et al. (2007), among others. In the Snow Lake deposits, the mineral is particularly abundant in the stringer ore zone (e.g., Franklin et al. 1981).

5.5 The ore deposit proper

Volcanogenic sulfide bodies of the bimodal-mafic type of oceanic arc settings usually feature a subsurface sulfide-silicate chimney or pipe consisting of a stringer and/or stockwork vein system and an overlying bulbous massive sulfide body. The pipe has a diameter generally smaller than, or equal to, that of the massive body, and a vertical extension up to 500 m or even more. Some stringer zones are actually much more voluminous than their related massive sulfide bodies. According to, e.g., Franklin (1993), stringer ore zones beneath all types of massive sulfide deposits are copper rich. Thus, in terms of composition and approximate size, the Chapada deposit conforms to a part of a volcanogenic system, namely the stringer zone, but lacks entirely the overlying

massive portion. That is to say, although located in an oceanic arc-type environment, which is permissive for the generation of a “complete” volcanogenic massive sulfide specimen, the deposit is essentially disseminated and the missing of a massive portion is arguably one of the most difficult aspects of Chapada to explain under a volcanogenic perspective. Yet regarding this, it could be contended that local geologic conditions could have prevented the generation of the massive sulfide facies. These conditions may include, for instance, unfocused upflow of the hydrothermal fluid, the presence of relatively porous host rocks, e.g., felsic tuffs and siliciclastic rocks, as well as the possible sealing effect of an impermeable cap rock. The treatment of these questions, however, involves aspects of the volcanogenic model that need to, and will be, addressed more thoroughly in the next section, on exhalites, as well as in the subsequent discussion items.

Meanwhile, to address specifically the aspect of original rock porosity, a summary of ore-hosting rocks as described by different authors has been provided, indicating a variety of views on the theme (Table 5). For Richardson et al. (1986), for instance, the ore host lithologies of Chapada constitute the wall-rock ensemble to a mineralizing intrusion. Kuyumjian (1989a, 1991) and Oliveira et al. (2004) in turn mention that the main host rocks, feldspathic biotite schist and feldspathic metasandstone, display the geochemistry of calc-alkaline dacites and have acid metatuffs as protoliths. For Oliveira (2009), the magnetite-biotite gneiss/muscovite-biotite schist on

the core of the NE portion of the deposit, corresponding to the so-called Capacete orebody, is derived from an intermediate to felsic plutonic rock, whereas the enveloping mineralized biotite-muscovite schist, metachert-metavolcaniclastic rock and amphibolite are part of a volcanic-sedimentary sequence. Kuyumjian et al. (2010) and Oliveira et al. (2016), in contrast, reinterpret the previously defined feldspathic metasandstone as a metafelsic to intermediate plutonic to subvolcanic rock, e.g., an equigranular metadiorite. Finally, for Moore et al. (2019), the most important host rocks of Chapada are fine-grained (muscovite-epidote)-biotite gneiss and amphibole-biotite gneiss. Whole rock geochemistry combined with petrography suggests an intermediate metavolcanic protolith for these rocks. According to these authors, intrusive gneissic rocks with porphyritic to equigranular texture and dioritic composition occur usually associated with the ore-hosting intermediate metavolcanic rocks throughout the deposit but are, nevertheless, mostly deprived of mineralization.

From the above summary, it may be concluded that interpretation of the nature of the host rocks of Chapada is somewhat controversial, with particular reference to the feldspathic biotite schist, the principal host rock, which has been interpreted as a dacitic tuff, a plutonic to subvolcanic diorite, or an intermediate volcanic rock. In any case, the ore host association has a significant contribution of rocks of the Mara Rosa sequence, including the mentioned metavolcanic and metavolcaniclastic rocks and metachert. Moreover, for

TABLE 5. Host rocks of the Chapada deposit according to different authors.

SOURCE	HOST ROCK	INTERPRETATIONS / OBSERVATIONS
Richardson et al. (1986)	Biotite schist is the most important ore-bearing rock of the deposit, hosting approximately 80% of the ore, with amphibolite and muscovite schist accounting for 10% each, and feldspathic quartzite hosting less than 1%	Host rocks considered walls to intrusion; amphibolite is ortho-derived (plagioclase phenocrysts), being either sub-volcanic or extrusive; homogeneity suggests subvolcanic; local abundance of Al-mineral such as kyanite and staurolite could reflect advanced argillic alteration
Silva and Sá (1988)	Quartz-feldspathic biotite schist with fine- to medium-grained siliceous matrix	Rock probably derived from felsic tuffs constituting a stratigraphic horizon
Kuyumjian (1989a, 1991)	Mainly feldspathic quartz-biotite schist and feldspathic metasandstone	Rock may constitute a metamorphosed dacitic tuff
	Staurolite-gedrite rock, pyritic quartz-sericite schist and quartzite (metachert) also contain some sulfides; epidote and epidote-rich amphibolite well-distributed just west of, and in contact with, the deposit	Two first rock types interpreted as chloritic (or exhalative mud) and phyllic alteration zones, respectively, and quartzite as metachert; epidote and epidote-rich amphibolite considered reaction root zone of hydrothermal cell
Oliveira et al. (2004)	Feldspathic biotite schist (80% of ore-bearing rock), sericite-rich schist (10%), gedrite-anthophyllite schist (10%) and a subordinate silicified zone	Feldspathic biotite schist referred to as of probable tuffaceous origin; mentioned rocks represent products of hydrothermal alteration
Oliveira (2009)	Antiform core with magnetite-biotite gneiss and muscovite-biotite schist flanked by amphibole schist, biotite-muscovite schists, metacherts, metavolcaniclastic rocks, kyanite-quartz schists and amphibolite bodies	Biotite gneiss core corresponds to a plutonic calc-alkaline felsic to intermediate plutonic body of a volcanic arc environment and the flanking rock association is related to a volcanic-sedimentary sequence
Kuyumjian et al. (2010)	Host rocks include a large variety of schists associated with magnetite-biotite gneisses and amphibolites, among which are outstanding: muscovite-biotite schists (60% of the total hosts), hornblende-anthophyllite-gedrite schists, an association of kyanite-staurolite-amphibole-garnet-biotite-muscovite schist, feldspathic kyanite-epidote-muscovite-biotite schist, metachert and an association of pyrite-bearing kyanite, quartz-kyanite, kyanite quartzite, kyanite-muscovite-quartz schist not strictly mineralized in copper, but locally containing some gold	Feldspathic metasandstone are interpreted as a metafelsic to intermediate intrusive or subvolcanic rock; staurolite-gedrite rocks as possible chloritic alteration; high-K biotite schist with microcline as potassic alteration; schist association considered volcanic-sedimentary, including volcaniclastic rocks and metacherts; kyanites and kyanite-quartz rocks considered metamorphosed advanced argillic alteration products related to a porphyry copper hydrothermal system
Oliveira et al. (2016)	Mineralization largely hosted by biotite-rich schist (biotite schist, muscovite-biotite schist, amphibole-biotite schist) and less so by biotite gneiss, epidote-amphibole schist, kyanite- and muscovite-rich schist and quartzite, including kyanites (cf. Table 1)	Biotite-rich schist superimposed on metadiorite and less so on volcanic-sedimentary rocks; former metasandstone reinterpreted as equigranular to porphyritic metadiorite; rock types interpreted as potassic, phyllic, argillic, advanced argillic and propylitic alteration of a porphyry copper hydrothermal system
Moore et al. (2019)	Epidote-muscovite-amphibole-biotite gneiss of the so-called A and B layers is the most important host rock (cf. Table 2)	Intermediate metavolcanic rock, based on geochemistry and petrography; alterations interpreted as Oliveira et al. (2016)

some authors, e.g., Moore et al. (2019), the intrusive rocks of the deposit are practically devoid of mineralization, an appreciation that agrees with the concept of a wall rock-hosted deposit of Richardson et al. (1986). A good deal of these rocks – as the primary volcanic and volcanoclastic rocks themselves - probably had adequate pre-lithification porosity to permit infiltration of mineralizing fluids. On top of this, two other aspects – the mentioned concept of a wall-rock hosted deposit (Richardson et al. 1986) and the hint that the tonalitic and dioritic gneisses are generally not mineralized (Oliveira et al. 2016, cf. Fig. 4; Moore et al. 2019) - suggest that the mineralization of Chapada is hosted predominantly in supracrustal rocks.

5.6 Exhalites, cap rocks and favorable ore horizons

Exhalites are common distal products of sea floor hydrothermal discharge. They are usually thin but typically extensive (10s of km), being made up usually of a chemical or hydrothermal component and a clastic or tuffaceous fraction. They represent an important indicator that hydrothermal activity took place during periods of volcanic quiescence and may precede, be synchronous with or post-date the VMS deposit formation.

Volcanogenic ore horizons typically grade laterally and vertically into thin ferruginous chert or sediment layers called informally “exhalites” (e.g., Franklin et al. 2005; Höy 1995). The horizon may include, for instance, chert, jasper, barite, carbonate, pyritic carbonaceous black shale, and gahnite quartzite where metamorphosed. It may consist of a particulate, e.g., Fe-Mn-rich, deposited from hydrothermal plumes and mixed with fine-grained sediment, so that the end exhalite may actually constitute a mixture of volcanoclastic, hydrothermal-chemical and epiclastic fractions. It may also exhibit a very variegated mineralogy depending on the grade of metamorphism, including quartz, Fe- and Mn-phases, pyrite, muscovite, biotite, barite, tourmaline, zincian staurolite, gahnite, apatite, garnet, epidote, kornepine, cordierite, sillimanite, corundum, aluminosilicates, sphene and anhydrite, among many others (e.g., Plimer 1986; Parr and Plimer 1993; Spry et al. 2000; Bonnet and Corriveau 2006, 2007; Slack 2012; Corriveau and Spry 2014). Relative predominance of some of these phases defines corresponding facies enriched in Si, Fe, Mn, Zn, B, Al, Ca, P or Ba, as indicated in Plimer (1986) and Parr and Plimer (1993) (Table 6). Some of these minerals, e.g., Zn-bearing silicates as zincian staurolite and the zincian spinel gahnite as well as Mn-garnet and chloritoid have been considered typical exhalative indicator minerals (Plimer 1986; Spry et al. 1998; Corriveau and Spry 2004). They occur as accessory phases, for instance, in volcanogenic chimneys. Gahnite in particular is present in virtually all volcanogenic deposits that attained amphibolite grade metamorphism (Franklin 1996) whereas zincian staurolite is cited specifically in connection with gold-rich volcanogenic deposits (Dubé et al. 2007).

According to Franklin et al. (2005), one important aspect related to the stratigraphic position of exhalites is that they commonly act to cap and protect the ore deposit. In some cases, the volcanogenic ore deposits may actually form underneath them, by lateral diffusion of hydrothermal fluid through permeable strata where the fluid is retained below the sea floor by the sealing effect of overlying impermeable materials such as chert or clay-silica altered products.

In the case of the Chapada – Mara Rosa area, the general occurrence of exhalites such as metachert, iron-formation and gondite in the Mara Rosa sequence is acknowledged for instance by Kuyumjian (1989a), Kuyumjian et al. (2010), Oliveira et al. (2014, 2016), Oliveira and Oliveira (2017) and Moore et al. (2019).

For the Chapada deposit in particular, Richardson et al. (1986) describe rocks composed essentially of magnetite and garnet as well as schists with abundant tourmaline interbedded in the ore-hosting sequence, which are referred to explicitly as exhalites by Kuyumjian (1991, 1995). Richardson et al. (1986) also indicate the occurrence in the deposit of gahnite and zincian staurolite (0.5-0.7 wt% ZnO) and mention that staurolite is preferentially concentrated in biotite schist, the most important ore host rock of the deposit. These phases have been considered typical exhalative indicator minerals, as mentioned earlier. Richardson et al. (1986) make the point that zones within all rock types of the Chapada deposit contain porphyroblastic zincian staurolite that makes up to 10 modal percent of the rock. Biotite schist and amphibolite are the most common staurolite-bearing lithologies. Still following these authors, although most metamorphic lithologies in the Chapada area are difficult to correlate, even between drill holes 50 m apart, ‘staurolite lithologies’ define local sub-horizontal

TABLE 6. Principal types of exhalites from Broken Hill, Australia (Parr and Plimer 1993; Plimer 1986).

TYPE	DOMINANT MINERALS	MINOR MINERALS
SILICEOUS	Quartz (commonly blue)	Spessartine, gahnite, sulfidites, tourmaline, magnetite, muscovite
MANGANIFEROUS	Spessartine-grossular, quartz	Apatite, gahnite, scheelite, sulfides, arsenopyrite, biotite, sillimanite, magnetite, piedmontite
FERRUGINOUS		
Sulfide facies	Pyrite, pyrrhotite, quartz	Muscovite, Ca-Fe pyroxene, fayalite, rhodonite
Carbonate facies	Ca-Mg pyroxene, quartz	Sulfides grossular-spessartine, epidote
Silicate facies	Grunerite, quartz	Magnetite, fayalite, sulfides, almandine-spessartine, stilpnomelane
Oxide facies		
Phosphatic	Magnetite, spessartine-grossular, quartz, apatite	Sulfides, fayalite, grunerite
Qz-magnetite	Quartz, magnetite	Barite, apatite, sulfides, sillimanite, muscovite
ZINCIAN	Gahnite, quartz	Sphalerite, Pb-orthoclase, spessartine-grossular, galena, sillimanite, apatite, tourmaline, muscovite, biotite, magnetite, ilmenite, ecantharsite, monazite
CALCAREOUS	Grossular, diopside, wollastonite, plagioclase, calcite, idocrase, quartz	Tremolite-actinolite, fluorite, graphite, epidote, scheelite, sphalerite, clinozoisite, sulfides, gahnite
BORON-RICH	Quartz, tourmaline	Feldspars, spessartine-almandine, biotite, muscovite, graphite, sillimanite, andalusite, apatite, sulfides, gahnite, magnetite, monazite

surfaces. This widespread and pervasive distribution of zincian staurolite certainly reflects a pre-metamorphic feature that can be interpreted as an exhalative zinciferous contribution of the local environment. Additionally, the fact that biotite schist, the main ore-hosting rock of Chapada, is the more important zincian staurolite-bearing lithology of the deposit argues strongly in favor of a volcanogenic origin of the ore itself.

A further mineral-related aspect of possible exhalative connection in Chapada is the occurrence of a finely banded iron-formation showing high density of garnet bands, e.g., with as much as seven garnet bands/cm (Kuyumjian 1989a). According to this author, this kind of finely banded garnet-rich iron-formation of Chapada is very similar to those of the Wilyama Complex, the stratigraphic unit that hosts the world-class exhalative Zn-Pb-Ag deposit of Broken Hill, in New South Wales, Australia.

Besides this, the occurrence in the Chapada pit of beds of sulfidic quartzite interpreted as metachert is acknowledged by Kuyumjian et al. (2010) and Oliveira et al. (2016) (Fig. 12). The rock is described as light to yellowish gray, massive to slightly banded, and made up of quartz with lesser muscovite, pyrite and chalcopyrite. The sulfides are relatively abundant in places (up to 10%) and occur as stretched grains that define a rough banding. Moreover, near the Chapada pit, a bed of gondite – another classical exhalite – has been mapped a few kilometers east of the deposit (Moore et al. 2019).

Additionally, the epidosite of Chapada, described originally by Kuyumjian (1989a), may also constitute an exhalative product. The rock has been described as a striped (i.e., banded) pale yellow-green lithotype composed of a mosaic of anhedral epidote, lobate quartz, sphene and subordinated magnetite with some bands containing almost only epidote and sphene (Kuyumjian 1989a, 1991, 1995). It occurs within the epidote-rich amphibolite zone (cf. section 5.2), but preferentially near the contact with the eastern metasedimentary unit, in the form of narrow, up to 5m-wide bands that compose a thin but persistent layer that runs for several kilometers just west of the Chapada deposit (Kuyumjian 1989a, b, 1991, 1998a) (Fig. 13).

It is speculated here that the Chapada epidosite, by virtue of its composition, banded texture and mode of occurrence as a thin and extensive layer represent a particular epidote-rich exhalite facies, following the diversity of composition of this kind of rock recognized, e.g., by Plimer (1986) and Parr and Plimer (1993, Table 6). To reinforce this interpretation an

example of occurrence of epidote-rich exhalites in Canada is presented in Bonnet and Corriveau (2006, p. 49), who have specifically recognized occurrences of this kind of rock in the Lac Musquaro region, Basse Côte-Nord, in the Quebec province of Canada. They describe a light-green, laminated quartzite showing discontinuous, millimeter-size epidote-rich bands with associated garnet (cf. their figure C of plate VII, p. 49) and accessory sphene (cf. p. 44). The rock has been interpreted in this case as a Mn-rich metaexhalite, but the abundance of epidote in the rock is evident from the mentioned figure itself.

If this interpretation holds for the epidosite of Chapada, this type of rock may indeed represent another evidence of the waning stage of a volcanic cycle or a hiatus in volcanic activity, representing the geological situation that has been recognized as the usual condition for the generation of volcanogenic deposits (e.g., Sangster 1972).

On top of all this, it may be argued that the sulfidic kyanite-muscovite quartzites and quartz schists of Chapada may consist of rocks with exhalative contribution and include even authentic metachert similar to those that have been recognized in the mine pit and environs, as mentioned above.

The peculiar high-alumina chemistry of these rocks, as expressed particularly by the abundance of kyanite, has been generally explained as resulting from an advanced argillic quartz-kaolinite alteration product that underwent metamorphism, without any further interpretation concerning the original unaltered protolith (e.g., Richardson et al. 1986; Nascimento et al. 2008; Kuyumjian et al. 2010; Moore et al. 2019). The nature of the pre-alteration rock, however, was in fact addressed by Costa (1984) (in Angeiras et al. 1988 and Arantes et al. 1991) and Oliveira et al. (2016). The former author considered the ultimate protoliths to be mafic volcanic rocks and intermediate tuffs submitted to a synvolcanic acid-leaching alteration process (see below). Oliveira et al. (2016) in contrast suggested that, due to the regional linear distribution of these kyanitic rocks in the Chapada – Mara Rosa region, the pre-alteration protoliths might have been porphyry dyke-like bodies. These two interpretation have good support in the literature. A general felsic volcanic protolith has been indicated for high-quartz-alumina hydrothermally altered rocks (e.g., Owens and Pasek 2007; Hedenquist 2010; Hedenquist and Taran 2013). Alteration occurs specifically through dissolution of aluminosilicates, feldspars in particular (e.g., Taylor 2007,



FIGURE 12. Outcrop (A) and hand sample (B) of metachert from the Chapada open pit (from Oliveira et al. 2016 and Kuyumjian et al. 2014, cf. figures 4C and 8E therein, respectively).

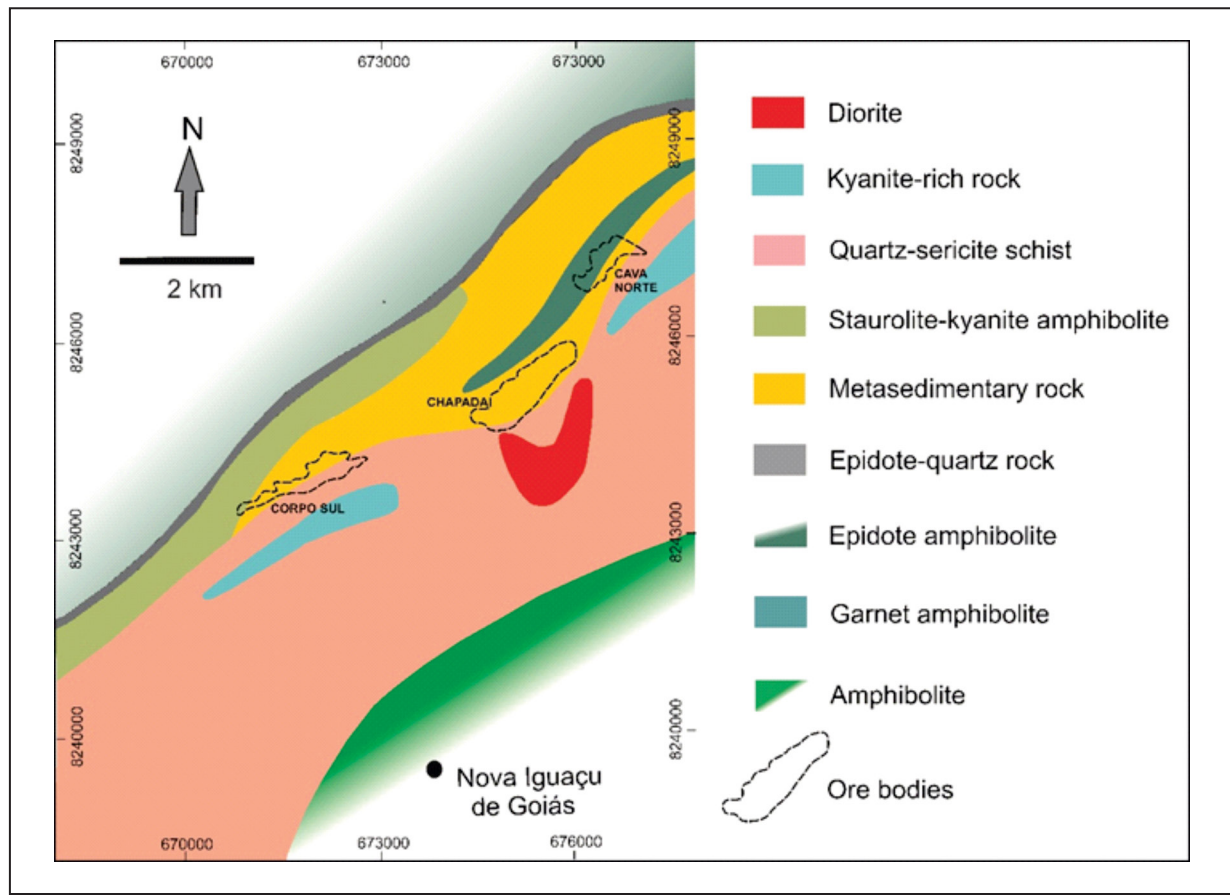


FIGURE 13. A simplified map showing the rock units of the hydrothermal zones of the Chapada area and, particularly, the morphology of the epidote-quartz, or epidosite, rock unit (from Kuyumjian 1989a). Fading limits indicate undefined contacts in the original illustration. Location of orebodies is approximate (from Oliveira et al. 2016, cf. Figure 4). Note the geologic differences between this map and those of figures 3 to 5, reflecting different authors and/or different stages of the mapping of the area.

p. 121; Jébrak and Marcoux 2014, p. 289), and leaching of most of the major elements of the host volcanic or volcanicsedimentary rock (Robb 2008, p. 118).

Notwithstanding, another interpretation is that the formation of the alumina-rich kyanite-muscovite quartzites and quartz schists rocks in Chapada and in the Mara Rosa region may have involved an exhalative contribution. To start with, these rocks contain varietal and accessory minerals such as rutile, muscovite, pyrite (\pm gold), biotite, corundum, tourmaline, lazulite, roscoelite (V-rich muscovite) and anhydrite, with associated quartz-sericite/muscovite-pyrite schists, and local zones enriched in sillimanite, kyanite, garnet, staurolite and chlorite (Angeiras et al. 1988; Arantes et al. 1991; Palermo et al. 2000; Kuyumjian et al. 2010). Furthermore, pyrite may occur in elevated concentrations (>10%) accompanied by some gold (Oliveira et al. 2016), so much so that a prospect, with gold hosted in an extensive belt of pyrite-rich kyanite-muscovite schist is actually located about 4 km east of Chapada (Miranda et al. 2018). The picture of high silica, sulfide concentrations and variegated accessory mineralogy is very remindful of exhalites, as formerly detailed in this section. Feldspar may have been added to the system by tuffaceous contribution or clastic input, providing in this way the alumina that was concentrated via hydrothermal leaching. Both chemical exhalative and tuffaceous products may coexist in the waning stages of the volcanic environment. Thus, one alternative interpretation for the peraluminous quartzites and

quartz schists of Chapada is that their protoliths consisted originally of a quartz-feldspathic rock formed as an epiclastic-tuffaceous-exhalative horizon, whose aluminum content was enhanced via syn-depositional hydrothermal acid leaching. This process somehow preserved the subtle chemical variations of the original rock horizon that are revealed via metamorphism by the variegated accessory mineralogy that characterizes exhalites.

This sedimentary connotation for the kyanite quartzites and associated rocks gains in significance if their possible role as cap rocks that might have induced sub-seafloor deposition of the Chapada ore is taken into consideration. In this respect, it is worth noting the widespread distribution of these rocks SE of the deposit, apparently in a hanging wall position. Oliveira et al. (2004), Oliveira (2009) and Kuyumjian et al. (2010, cf. Fig. 3), for instance, in their semi-detail maps, show that lenses of quartzite and kyanitites extend for ca. 15 km along strike in the Chapada deposit area, with some lenses lying in direct contact with the deposit itself. Miranda et al. (2018) suggest that in a pre-deformation configuration these rocks could have been located atop the Chapada deposit. These aspects, along with the geometry, extension and presumably hanging wall position of these rocks, suggest their possible 'capping role' in relation to the Chapada deposit as pointed out in the last section, that is, they may have acted as a sealing blanket that forced the sub-seafloor metal deposition from Chapada's hydrothermal fluid. The mentioned exhalative nature and stratigraphic

position of these rocks are reinforced by the occurrence of a gondite horizon also east of Chapada (cf. Moore et al. 2019, Fig. 7.3 therein), a rock of exhalative nature, which commonly occurs stratigraphically above volcanogenic sulfide bodies.

Linked with the above-discussed exhalite concept is the notion of favorable, or equivalent, ore horizon of Sangster (1972) and Large (1992). According to these authors, exhalite is a characteristic sediment that commonly defines the favorable, or ore equivalent, horizon within the host volcanic pile, forming a marker unit for mapping and exploration. Large (1992) actually defines seven of these ore-equivalent horizons for the case of Australian VMS deposits. The horizons may include, for instance, chert, jasper, barite, carbonate, gahnite quartzite and pyritic carbonaceous black shale.

In our view, a case for an example of one or more favorable ore horizons can be made in connection with the regional elongated segments of aluminous rock bodies of the Chapada – Mara Rosa region, which extend for about 100 km (cf. Fig. 2).

Regarding this, among specific ore-equivalent volcanogenic strata, Large (1992) describes examples consisting of gahnite quartzite, pyritic quartzite and siltstone, and fine-grained rhyolitic epiclastics, which, in part, resembles the protolithic horizon preconized above for the peraluminous muscovite-kyanite-quartz rocks of Chapada.

6 Further discussions and conclusion

As mentioned before, there is no intention here of making any appraisal of 'non-volcanogenic' models that have been applied to Chapada, i.e., wall-rock porphyry, porphyry-epithermal, orogenic and intrusion-related. For a succinct review of the subject, one should refer particularly to Table 7 below and references therein.

As stated earlier, the scope of the present exercise has been to emphasize that, despite other models that have been proposed, a good deal of the features of Chapada and its hosting geologic setting can also be viewed in terms of, and used in support of, a volcanogenic model. Regarding this,

Table 8 and Figure 14 are presented below to show, summarily and respectively, (1) the adherence of selected features of Chapada to the essential attributes of the volcanogenic model, based on data compiled in sections 4 and 5; and (2) the close and organic geologic relation between these attributes according to the general model for volcanogenic deposits presented, e.g., in Franklin et al. (2005), Galley et al. (2007) and Gibson et al. (2007).

Additionally, there are further aspects related to the aluminous hydrothermal alteration and the disseminated nature of Chapada that deserve further discussion in connection with the volcanogenic model.

Regarding the aluminous alteration - which has been interpreted as advanced argillic alteration of a high-sulfidation lithocap atop a porphyry hydrothermal system (e.g., Nascimento et al. 2008; Kuyumjian et al. 2010; Oliveira et al. 2016; Miranda et al. 2018; Moore et al. 2019) – it should be emphasized that the feature is not exclusive of the porphyry-epithermal environment. On the contrary, as exemplified in section 5.4, this very same alteration feature may also occur in association with volcanogenic deposits, in particular those developed under relatively shallow water conditions. So much so that, by analogy with epithermal deposits, these shallow-water deposits and their deeper water analogs have been coined high- and low-sulfidation volcanogenic deposits, respectively, by Sillitoe et al. (1996) and acknowledged as such by Hannington et al. (1999) and Dubé et al. (2007) (cf. Fig. 15). High-sulfidation VMS deposits may in fact display advanced argillic alteration and gold enrichment similarly to epithermal deposits, and yet exhibit clear volcanogenic attributes (Franklin 1996).

Accordingly, Bonnet and Corriveau (2006, 2007) and Dubé et al. (2007), for instance, state that the presence of aluminous alteration marked by distinct mineral assemblages, containing pyrophyllite, andalusite, corundum, kyanite and sillimanite, constitute a useful exploration guide to Au-enriched volcanogenic deposits in metamorphic terranes, whereas Franklin (1996) adds that aluminous alteration can also occur

TABLE 7. A synopsis of metallogenic models proposed historically for the Chapada deposit.

PROPOSERS	MODEL	OBSERVATIONS
Richardson et al. (1986)	Wall rock-hosted porphyry copper	Feeder zone of VMS deposit seen as a possibility (p. 1895)
Silva and Sá (1988)	Volcanogenic	Possible remobilization through subsequent shearing
Kuyumjian (1989a)	Volcanogenic disseminated	Probable deposition on to the seafloor (p. 203)
Kuyumjian (1991)	Hydrothermal exhalative	Extensive metamorphogenic redistribution
Kuyumjian (1995, 1998)	Volcanogenic exhalative with meta-morphic redistribution	Contribution of hydrothermal fluids from diorite-tonalitic intrusions (that leached metals from favorable source rocks and pervaded the earlier mineralized hydrothermal zone (1995, p. 204)
Kuyumjian 2000	Volcanogenic(?) exhalative (abstract) with magmatic contribution (p. 287)	Metamorphosed porphyry-epithermal system related mineralization (p. 287)
Oliveira et al. (2000, 2004)	Porphyry copper, related to early, oceanic arc subduction stage or orogenic development (2000, p. 221)	Hydrothermal alteration processes coeval with or post-date the main Neoproterozoic deformation during the Basiliano orogeny (2004, p. 297)
Ramos Filho et al. (2003)	Orogenic remobilization	Mineralization associated with D2 deformational event and related retrograde metamorphism
Ramos Filho et al. (2005)	Epithermal-porphyry copper	Following Kuyumjian (2000)
Oliveira (2009), Kuyumjian et al. (2010)	Partly porphyry copper and partly granite-related.	Granite-related model applied to the so-called Capacete sector of the deposit.
Oliveira et al. (2014, 2016)	Partly porphyry copper and partly granite-related. Epithermal gold.	Epithermal gold in advanced argillic alteration representing lithocap of porphyry system
Moore et al. (2019)	Porphyry copper with remobilization by orogenic fluids	Reference to early-, late inter- and late-mineral porphyry intrusions

TABLE 8. Degree of congruity between essential attributes of the volcanogenic model and the Chapada deposit. Numbers refer to items in section 5 and location of attributes in figure 14.

Essential (1-6) & other volcanogenic attributes	Degree of Chapada's adherence / Main aspects
1- Magmatic granitoid heat source	Moderate / Age gap of 20 Ma to nihil relative to VS sequence
2- Semi-conformable regional alteration zone	High / Mapped regionally immediately west of Chapada
3- Synvolcanic faulting	Moderate / Adequate fault systems that can fit the model
4- Deposit-scale hydrothermal alteration zone	High / Chloritic, sericitic, aluminous and propylitic halos
5- Volcanogenic orebody proper	Low / Disseminated ore only, no massive sulfide facies
6- Exhalite products / Cap rock	High / Chert, BIF, gondite, mixed clastic-exhalite-tuffaceous rocks(?)
Favorable or equivalent ore horizon	Moderate / Regionally distributed Al-rich quartzites and schists
Tectonic setting	High / Oceanic arc, bimodal VS sequence, synvolcanic(?) plutons

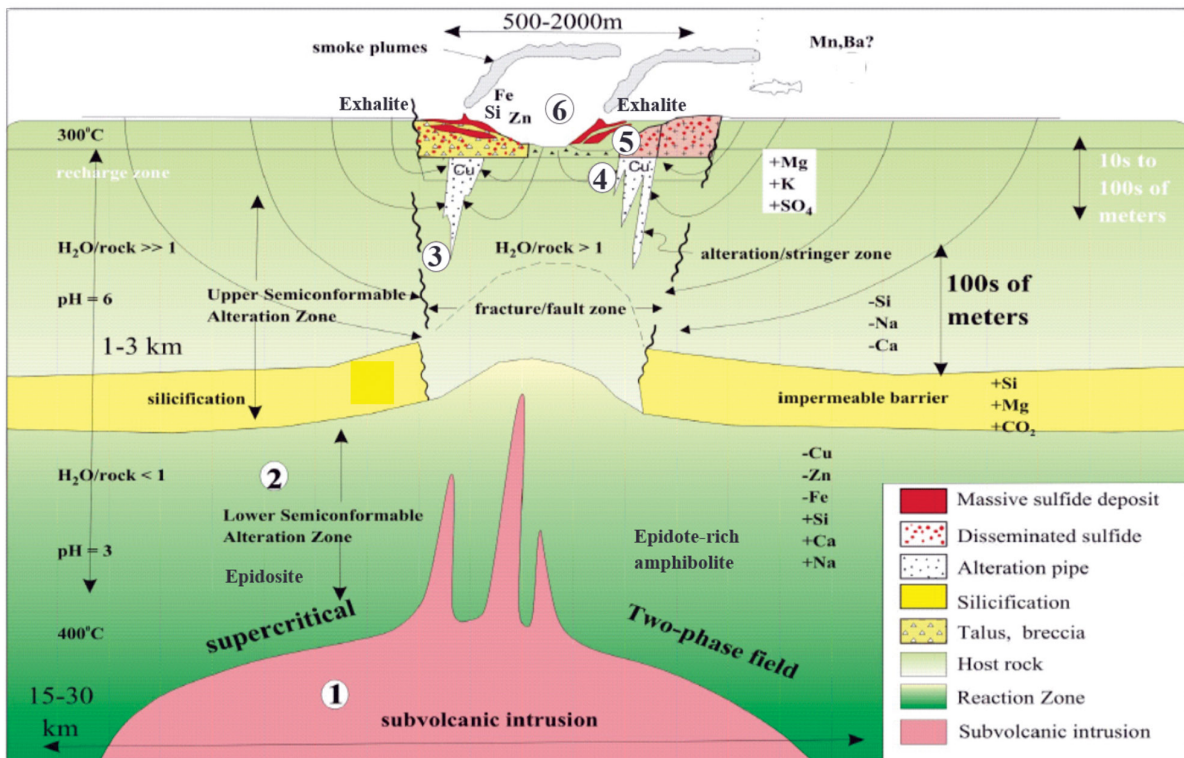


FIGURE 14. Schematic illustration showing the essential attributes (1 to 6) of the geologic setting of a volcanogenic deposit as discussed in sections 5.1 to 5.6 in the text (modified from Gibson et al. 2007).

in conventional, base metal-rich and gold-poor volcanogenic deposits. A good example in the Mara Rosa Arc of a gold-enriched VMS deposit with associated aluminous alteration is the Zacarias deposit, located ca. 40 km northwest of Chapada. At Zacarias, the bulk of the gold ore is hosted in a sulfidic, gahnite-magnetite-bearing, barite-rich metachert, which is coeval, and partly intercalated, with massive sulfides. The ore contains silver, pyrite and sphalerite, with lesser galena and chalcopyrite. The metachert occurs atop a sequence of, mainly, basaltic to andesitic metatuffs that are intensely altered to aluminous-magnesian schists with complex mineralogy consisting of biotite, phlogopite, sillimanite, kyanite, staurolite, cummingtonite, anthophyllite and talc (Arantes et al. 1991; Pöll 1994, in Palermo et al. 2000; Oliveira et al. 2004, 2014).

This picture altogether is strongly reinforced by the occurrence of active submarine volcanic hydrothermal systems exhibiting advanced argillic alteration and associated Cu-Zn-Au mineralization, as exemplified in the Brothers

volcano caldera of the Southern Kermadec Arc, offshore New Zealand (de Ronde et al. 2005, 2019). The alteration assemblage consists of illite + amorphous silica + natroalunite + pyrite + native S, with associated plumes showing high concentrations of particulate copper. The site is interpreted as a nascent magmatic-hydrothermal system venting acidic waters related to the input of magmatic fluids. The caldera also hosts evolved seawater-dominated vent sites, with episodic magmatic fluid contribution, which have associated copper and zinc sulfides, and gold. The various vents are considered components of an evolving hydrothermal system typical of submarine volcanic Arcs whereas, quoting de Ronde et al. (2019), the high Cu-Au contents and strongly acidic fluids in these systems are similar to those that formed in the shallow parts of some porphyry copper and epithermal gold deposits mined today on land. Interestingly, a two-step evolution of the hydrothermal system is proposed by de Ronde et al. (2019). First an initial hydrothermal system, dominated by magmatic

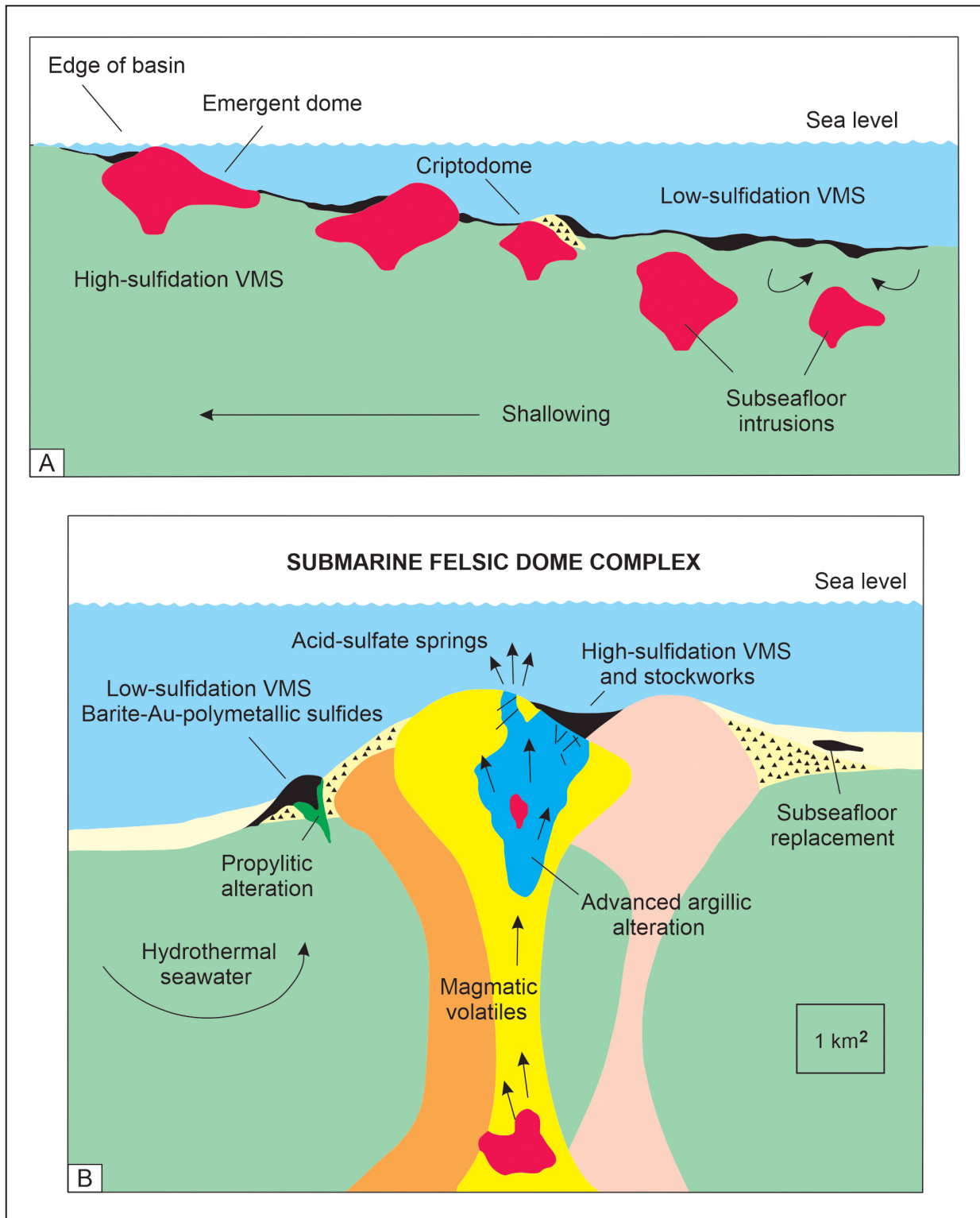


FIGURE 15. Schematic sections showing: A- the development of high-sulfidation versus low-sulfidation conditions in a submarine setting in relation to the depth of associated subvolcanic intrusion; B- the position of high- and low-sulfidation VMS environments in relationship to a submarine volcanic setting, with particular reference to the development of advanced argillic alteration (from Hannington et al. 1999 and Sillitoe et al. 1996, respectively; both in Dubé et al. 2007, modified).

fluids and highly saline brines, which remains sequestered in the subsurface, in a situation perhaps similar to Chapada's. This system is later on partly scavenged by the evolved seawater fluid, which upflows to form Cu-Zn-Au-rich chimneys at or near the seafloor. Zacarias may conceivably correspond to this latter situation.

The Suruca gold-only deposit has also has a metallic association, Au-(Ag-Pb-Zn) (Silva et al. 2011) that is similar to that of Zacarias and to the above-mentioned evolved seawater system of de Ronde et al. (2019). The deposit is hosted mostly in a Chapada-correlated metasedimentary, staurolite- and gedrite-bearing, garnet-amphibole/biotite-

quartz schist unit with disseminated pyrrhotite and lesser pyrite veinlets. However, differently from Zacarias, Suruca gold-only is a vein-type deposit. It occurs in a zone with an important increase of 'calcic' (garnet, amphibole, epidote, zoisite, quartz, carbonate and pyrite) veins and polymetallic (quartz, biotite, pyrite, sphalerite and galena) veinlets, accompanied by a parallel increase in epidote and sericite content. Gold is mostly associated with pyrite, although an association with zinc is also referred to (Moore et al. 2019).

The above observations, collectively considered, involve in fact an interesting corollary for Chapada and the Mara Rosa Arc. If one ponders the different scenarios entailed in epithermal (subaerial) versus volcanogenic (submarine) settings, the advanced argillic alteration of Chapada – being associated with rocks deposited in an oceanic basin – is much more likely to be related to an underwater, volcanic-exhalative environment than to the sub-aerial conditions of an epithermal system, nonetheless still maintaining the connection with an epizonal intrusion (cf. Fig. 15A).

To reinforce this corollary, it can be added that Al-rich kyanite / sillimanite quartzites perhaps similar to those of Chapada – Mara Rosa may form regional stratiform bodies in volcanic-sedimentary settings. A major example occurs in the Proterozoic Namaqua belt, South Africa, where sillimanite quartzites occur coevally with exhalites of siliceous, B-rich, zincian, calcareous, ferruginous and phosphatic composition (Willner et al. 1990; see also Ihlen 2000 and Müller et al. 2007). In the Appalachian Kings Mountains belt, e.g., Pinnacle, Gaston County, North Carolina, stratiform kyanite quartzites of a volcanic-sedimentary sequence grade into quartz-pebble metaconglomerates (Horton Jr. 1989; Ihlen 2000), indicating in this way their syn-depositional nature. Considering these examples, the extent of the kyanite-bearing quartzites and quartz schist of the Chapada – Mara Rosa region is more consonant with a regional, stratigraphy-related protolith than in much more localized hydrothermal products as in the case of epithermal lithocaps. As mentioned earlier, this situation is quite remindful of true favorable, or equivalent, ore horizons that are found in volcanogenic environments (Sangster 1972; Large 1992).

Back to the concern with the lack of a massive facies at Chapada, it could be also argued straightforwardly that there are examples among volcanogenic deposits of 'disseminated-only' deposits. One of such deposits is Prince Lyell, in the Mount Lyell district, Tasmania. In its lifetime (to 2002), the district has produced about 1.4 Mt of copper, 45 t of gold and 733 t of silver from about 120 Mt of volcanogenic 'non-massive sulfide' ore. Prince Lyell with ca. 90 Mt of disseminated Cu-Au ore is the only present producer and, depending on good metal prices, there are sufficient reserves to enable the mine continuing for another fifty years or more. The deposit is thought to have formed by sub-seafloor deposition from the unfocused upflow of solutions that percolated laterally permeable horizons of volcanoclastic breccias and sandstones lying underneath lesser exhalative massive sulfide deposits (Markham 1968; Walshe and Salomon 1981; Corbett 2001; Large 2002; Mindat 2019). The upper part of the alteration zone associated with the disseminated mineralization is characterized by numerous cherty silica masses contained within sericite-pyrite-silica schists, culminating in a very large chert body that appears to have formed a siliceous cap to the system (Corbett 2001). Prince Lyell demonstrates that a volcanogenic hydrothermal

edifice can generate a sizable disseminated deposit without necessarily the presence of a massive facies, and represents in our view an interesting volcanogenic template for the 'disseminated-only' nature of Chapada.

In agreement with this example, it has become clearer lately that many massive sulfides are actually deposited in sub-seafloor conditions, where a disseminated texture is more likely to develop, particularly within lithofacies dominated by volcanoclastic and/or terrigenous clastic sedimentary rocks (e.g., Franklin et al. 2005 p. 545; Gibson et al. 2007, p. 724). An important aspect to promote this kind of situation is a poorly-focused hydrothermal discharge under an impermeable cap rock package that forces lateral diffusion of the hydrothermal fluid instead of a channeled escape upwards. Processes such as infiltration, precipitation of sulfide in pore spaces and replacement have been invoked to promote mineralization under these conditions. This would even provide a more efficient mechanism to trap a higher proportion of metals compared to seafloor venting. The above-mentioned mechanism would lead to the development of relatively large (gold)-copper-bearing footwall alteration zones spreading away from synvolcanic fault conduits, constituting strata-bound and locally stratiform mineralized bodies, with width to depth ratios of up to 10:1 (Franklin et al. 2005). In addition, and more important to the present exercise, sub-seafloor volcanogenic sulfide deposit generation may have no, or only minor, associated exhalative counterpart (e.g., Gibson et al. 2007 and references therein). As already mentioned, Corbett (2001) describes an example of such situation specifically with respect to the Prince Lyell Cu-Au volcanogenic disseminated deposit.

In connection with the aspects above, it is significant to note that the host rock package of Chapada, consisting to a significant extent of intermediate metavolcanic and volcanoclastic rocks (e.g., Kuyumjian 1991; Kuyumjian et al. 2010; Moore et al. 2019), probably had originally the adequate permeability and composition for lateral fluid infiltration and, perhaps, sulfide replacement. It is also worth noting that these are conditions that, anyway, practically any subsurface deposition model proposed for the deposit should cope with. Besides this, it is worth noting as well that the quartzites that occur east of, and presumably stratigraphically above, the Chapada orebody may conceivably have performed the role of an impermeable cap rock, as already mentioned previously in sections 5.5 and 5.6.

Accordingly, considering these features and the material compiled in the former sections, it is suggested here as a working hypothesis that Chapada may correspond to a sub-seafloor stringer or disseminated facies of a volcanogenic hydrothermal system that failed to vent out and ended up generating an inhalative instead of a truly exhalative deposit in the strict meaning of the term.

To complete the present exercise, it is interesting and perhaps ironical to note that the sub-seafloor volcanic-related depositional setting was considered as an alternative interpretation for Chapada by Richardson and co-workers (1986, p. 1895), and reappeared in the literature only 25 years later in a brief reference by Kuyumjian et al. (2010, p. 66). Thus, the present volcanogenic contention constitutes actually a resumption of a theme that somehow lost appeal in the two last decades or so. Overall, the data compiled and discussed in this article make clear that essential volcanogenic features are well represented in Chapada and its geologic setting, and

should be considered in the metallogenic modeling of the deposit. In our view, mineralization was emplaced in a site with good evidence of volcanic-associated activity, probably in inhalative, sub-seafloor conditions. Regarding this, it is worth pointing out once more that host rocks of Chapada consist partly or even significantly of supracrustal lithologies and that the causative plutonic rocks of the almost unanimously accepted porphyry-copper model seem mostly unmineralized.

Finally, by way of a crude supplementary comparison of the applicability to Chapada of the two main types to which the deposit has been compared to – porphyry and volcanogenic – it should be noted that there is a relatively lack of constraining data critical to promote this balance on a sound basis. The main information available is principally of geologic nature, e.g., on tectonic setting, lithology, ore characterization and attending hydrothermal alteration – and can be ultimately ascribed to both deposit types. This twofold appraisal of Chapada's information applies even to stable isotope studies, to date restricted to sulfide sulfur isotope data. These return results close to zero per mil, which have been rightfully used as indicative of a magmatic origin of the mineralizing fluid and, therefore, as an argument in support of the porphyry type (Richardson et al. 1986, Oliveira et al. 2016), but which are equally usually obtained from Precambrian VMS deposits (e.g., Huston 1999, Franklin et al. 2005). On the other hand, one possibly very significant piece of information on Chapada concerning specifically the porphyry model is the identification in the potassic zone of the deposit of deformed veinlets similar to those known in porphyry systems as A-type (magnetite-chalcopyrite-bearing biotite quartz veinlets) and partly dissolved anhydrite veinlets, also found in these systems (Oliveira et al. 2016). In addition to these, Moore et al. (2019) report transposed sericite-pyrite D-type veinlets that would also be typical of porphyries in both the potassic and phyllic zones of Chapada. In terms of volcanogenic systems, it can perhaps be argued that silicification is commonly well developed, and less so sericitization, in sulfide stockworks, stringers and disseminations of chimneys of volcanogenic deposits (e.g., Franklin 1996, p. 178; Galley et al. 2007, p. 155; and section 5.4). Additionally, it should be noted that shear-related (D_{n+1}), sulfide-biotite-bearing quartz segregations have been recognized at Chapada (Kuyumjian et al. 2010, p. 64-65, Figure 11B therein; Oliveira 2009, p. 72, Figure 4.22 therein). Anyway, notwithstanding this and the foregone, perhaps arguable, points of the present comparative exercise, it is our final contention here that the possibility of Chapada constituting a deposit of the volcanogenic type should be brought back into discussion. This perspective should return to the ongoing metallogenic analysis of the deposit.

Acknowledgements

Thanks are due firstly and foremost to Ana Maria Dreher for the critical reading of the manuscript. Significant improvements in both geology and English writing were gained through her revision. She also contributed with the amphibolite facies column of Table 4, completing it conveniently in this way. Evandro Klein and Roberto Dall'Agnol are also acknowledged for their orientation on editorial and submission aspects. Christina Ransom deserves recognition for obtaining publisher's permission to use some of the figures and tables presented in the text. The author has equally a debt

of gratitude to librarians Flaslendo Oliveira and Anderson Santana for providing literature sources used in the present article. My thanks go to Jennifer Bates and Melanie Marshall as well for sorting out matters with SEDAR, to Mark Turner and Brian Middleton for replying messages to Lundin Mining, and to Jifril Balansag and Ralph Salimbagat for their help in the attempt of clearing up questions with Elsevier. Additionally, the effort of the reviewers – John Ridley, Mariana Brando Soares and an anonymous party – to improve many aspects of the article has been greatly appreciated, with particular recognition of John's examination of the manuscript with a fine-tooth comb. Last but not least, the checking of references carried out by Gabriela Leitão is also much recognized.

References

- Angeiras A.G., Costa L.A.M., Santos R.C. 1988. Depósito de ouro de Mara Rosa, Goiás. In: Schobbenhaus C., Coelho C.E.S. (coords.) Principais depósitos minerais do Brasil: volume III: metais básicos não-ferrosos, ouro e alumínio. Brasília, DNP/CMVRD. p. 523-534. Available on line at: http://acervo.cprm.gov.br/rpi_cprm/docreaderNET/DocReader.aspx?bib=PUBLICACOES_DNP&PagFis=76550 / (accessed on 5 May 2021)
- Arantes D., Osborne G.A., Buck P.S. 1991. The Mara Rosa volcano-sedimentary sequence and associated gold mineralization. In: Ladeira E.A. (ed.) Brazil Gold '91. Rotterdam, A. A. Balkema, p. 221-229.
- Barrie C.T., Hannington M.D. (eds.). 1999. Volcanic-associated massive sulfide deposits: processes and examples in modern and ancient settings. Reviews in Economic Geology, 8. Littleton, Colorado, Society of Economic Geologists. <https://doi.org/10.5382/Rev.08>
- Bonnet A.-L., Corriveau L. 2006. Atlas et outils de reconnaissance e systèmes hydrothermaux métamorphisés des les terrains gneissiques. Université du Québec / Institut National de la Recherche Scientifique / Ressources Naturelle Canada, 95 p. Available online at: <https://numerique.banq.qc.ca/patrimoine/details/52327/2316039> / (accessed on 20 April 2021).
- Bonnet A.-L., Corriveau L. 2007. Alteration vectors to metamorphosed hydrothermal systems in gneissic terranes. In: Goodfellow W.D. (ed.). Mineral deposits of Canada: a synthesis of major deposit-types, district metallogeny, the evolution of geological provinces, and exploration methods. Geological Association of Canada, Mineral Deposits Division and Geological Survey of Canada, Special Publication, 5. p. 1035-1049.
- Corbett K.D. 2001. New mapping and interpretation of the Mount Lyell mining district, Tasmania: a large hybrid Cu-Au system with an exhalative Pb-Zn top. Economic Geology, 96(5), 1089, Abstract. <https://www.doi.org/10.2113/gsecongeo.96.5.1089>
- Corriveau L., Spry P.G. 2014. Metamorphosed hydrothermal ore deposits. In: Holland H.D., Turekian K.K. Treatise on geochemistry. 2nd. ed. Amsterdam Elsevier. p. 175-193. <https://doi.org/10.1016/B978-0-08-095975-7.01107-4>
- Costa L.A.M. 1984. A comparison between the Hemlo gold province, Ontario, Canada with special reference to the Corona deposit and the Posse gold occurrences, Mara Rosa, Goiás, Brazil. Relatório MCL-576 Rio de Janeiro, Mineração Colorado Ltda.
- Dantas E.L., Jost H., Fuck R.A., Brod J.A., Pimentel M.M., Meneses P.R. 2001. Proveniência e idade deposicional de seqüências vulcano-sedimentares da região de Santa Terezinha de Goiás, baseada em dados isotópicos Sm-Nd em monocristal de zircão. Revista Brasileira de Geociências, 31(3), 329-334. <https://doi.org/10.25249/0375-7536.2001313329334>
- de Ronde, C.E.J., Hannington M.D., Stoffers P., Wright J.C., Ditchburn R.G., Reyes A.G., Baker E.T., Massoth G.J., Lupton J.E., Walker S.L., Greene R.R., Soong C.W.R., Ishibashi J., Lebon G.T., Bray C.J., Resing J.A. 2005. Evolution of a submarine magmatic-hydrothermal system: Brothers volcano, southern Kermadec Arc, New Zealand. Economic Geology, 100(6), 1097, Abstract. <https://doi.org/10.2113/gsecongeo.100.6.1097>
- de Ronde C.E.J., Humphris S.E., Höfig T.W., Reyes A.G. 2019. Critical role of caldera collapse in the formation of seafloor mineralization: The case of Brothers volcano. Geology, 47(8), 762, Abstract. <https://doi.org/10.1130/G47862a1>

- [org/10.1130/G46047.1](https://doi.org/10.1130/G46047.1)
- Dixon C.J. 1981. Atlas of economic mineral deposits. Ithaca, Cornell University Press, 143 p. <https://doi.org/10.1007/978-94-011-6511-2>
- Dubé B., Gosselin P., Mercier-Langevin P., Hannington M., Galley A. 2007. Gold-rich volcanogenic massive sulphide deposits. In: Goodfellow W.D. (ed.). Mineral deposits of Canada: a synthesis of major deposit-types, district metallogeny, the evolution of geological provinces, and exploration methods. Geological Association of Canada, Mineral Deposits Division and Geological Survey of Canada, Special Publication, 5, p. 75-94.
- Eckstrand O.R., Sinclair W.D., Thorpe R.I. (eds.). 1995. Geology of Canadian Mineral Deposit Types. Geology of Canada, 8. Ottawa, Geological Survey of Canada, 640 p. <https://doi.org/10.1130/DNAG-GNA-P1>
- Eckstrand O.R., Sinclair W.D., Thorpe R.I. 1996. Introduction. In: Eckstrand O.R., Sinclair W.D., Thorpe R.I. (eds.). 1995. Geology of Canadian Mineral Deposit Types. Geology of Canada, 8. Ottawa, Geological Survey of Canada. p. 1-7. <https://doi.org/10.1130/DNAG-GNA-P1>
- Franklin J.M. 1993. Volcanic-associated massive sulphide deposits. In: Kirkham R.V., Sinclair W.D., Thorpe R.I., Duke J.M. (eds.). 1993. Mineral deposit modeling. Geological Association of Canada Special Paper, 40. Stittsville, Ontario, Geological Association of Canada. p. 315-334.
- Franklin J.M. 1996. Volcanic-associated massive sulphide base metals. In: Eckstrand O.R., Sinclair W.D., Thorpe R.I. (eds.). 1995. Geology of Canadian Mineral Deposit Types. Geology of Canada, 8. Ottawa, Geological Survey of Canada. p. 158-183. <https://doi.org/10.1130/DNAG-GNA-P1>
- Franklin J.M., Gibson H.L., Jonasson I.R., Galley A.G. 2005. Volcanogenic massive sulfide deposits. In: Hedenquist J.W., Thompson J.F.H., Goldfarb R.J., Richards J.P. (eds.). 2005. Economic Geology: One Hundredth Anniversary Volume: 1905-2005. Littleton, Colorado, Society of Economic Geologists. p. 523-560. <https://doi.org/10.5382/AV100.17>
- Franklin J.M., Lydon J.W., Sangster D.M. 1981. Volcanic-associated massive sulfide deposits. In: Skinner B.J. (ed.). Economic Geology: Seventy-Fifth Anniversary Volume: 1905-1980. Lancaster, Pennsylvania, The Economic Geology Publishing Company. p. 485-627. <https://doi.org/10.5382/AV75.15>
- Galley A.G. 1993. Characteristics of semi-conformable alteration zones associated with volcanogenic massive sulphide districts. Journal of Geochemical Exploration, 48(2), Abstract. [https://doi.org/10.1016/0375-6742\(93\)90004-6](https://doi.org/10.1016/0375-6742(93)90004-6)
- Galley A. 2002. Characteristics of composite subvolcanic intrusive complexes associated with Precambrian VMS districts. In: Galley A., Bailes A., Hannington M., Holk G., Katsube J., Paquette F., Paradis S., Santaguida F., Taylor B., Hillary B. Database for CAMIRO Project 94E07: interrelationships between subvolcanic intrusions, large-scale alteration zones and VMS deposits, Geological Survey of Canada, Open File 4431. p. 1-40. <https://doi.org/10.4095/213755>
- Galley A. 2003. Composite synvolcanic intrusions associated with Precambrian VMS-related hydrothermal systems. Mineralium Deposita, 38, 443-473. <https://doi.org/10.1007/s00126-002-0300-9>
- Galley A.G., Bailes A.H., Kitzler G. 1993. Geological setting and hydrothermal evolution of the Chisel Lake and North Chisel Zn-Pb-Cu-Ag-Au massive sulfide deposits, Snow Lake, Manitoba. Exploration and Mining Geology, 2(4), 271-295. Available online at: <https://pubs.geoscienceworld.org/cim/emg/article/2/4/271/61028/Geological-setting-and-hydrothermal-evolution-of> / (accessed on 30 April 2021)
- Galley A.G., Hannington M.D., Jonasson I.R. 2007. Volcanogenic massive sulphide deposits. In: Goodfellow W.D. (ed.). Mineral deposits of Canada: a synthesis of major deposit-types, district metallogeny, the evolution of geological provinces, and exploration methods. Geological Association of Canada, Mineral Deposits Division and Geological Survey of Canada, Special Publication, 5, p. 141-161.
- Gibson H.L., Allen R.L., Riverin G., Lane T.E. 2007. The VMS model: Advances and application to exploration targeting. In: Milkereit B. (ed.) Proceedings of Exploration 07: Fifth Decennial Conference on Mineral Exploration. p. 713-730. Available online at: <http://www.dmecc.ca/ex07-dvd/E07/pdfs/49.pdf> / (accessed on 01 July 2017).
- Goodfellow W.D. (ed.). 2007. Mineral deposits of Canada: a synthesis of major deposit-types, district metallogeny, the evolution of geological provinces, and exploration methods. Geological Association of Canada, Mineral Deposits Division and Geological Survey of Canada, Special Publication, 5, 1061 p.
- Goodfellow W.D., Lydon J.W., Turner R.J.W. 1993. Geology and genesis of stratiform sediment-hosted (SEDEX) zinc-lead-silver sulphide deposits. In: Kirkham R.V., Sinclair W.D., Thorpe R.I., Duke J.M. (eds.). 1993. Mineral deposit modeling. Geological Association of Canada Special Paper, 40. Stittsville, Ontario, Geological Association of Canada. p. 201-251.
- Goodfellow W.D., McCutcheon S.R., Peter J.M. 2003. Massive sulfide deposits of the Bathurst Mining Camp, New Brunswick and Northern Maine: Introduction and summary of findings. In: Goodfellow W.D., McCutcheon S.R., Peter J.M. (eds.), Massive Sulfide Deposits of the Bathurst Mining Camp, New Brunswick, and Northern Maine. Economic Geology Monograph 11, Society of Economic Geologists, p. 1-16. <https://doi.org/10.5382/Mono.11>
- Hagemann S.G., Brown P.E. (eds.). 2000. Gold in 2000. Reviews in Economic Geology, 13. Littleton, Colorado, Society of Economic Geologists, 559 p. <https://doi.org/10.5382/Rev.13>
- Hannington M.D., Poulsen K.H., Thompson J.F.H., Sillitoe R.H. 1999. Volcanogenic gold in the massive sulfide environment. In: Barrie C.T., Hannington M.D. (eds.). Volcanic-associated massive sulfide deposits: processes and examples in modern and ancient settings. Reviews in Economic Geology, 8. Littleton, Colorado Society of Economic Geologists. p. 325-356. <https://doi.org/10.5382/Rev.08.14>
- Hedenquist J.W. 2010. Formation of advanced argillic lithocaps over porphyry systems, and implication for exploration. GSA Annual Meeting & Exposition, Paper No. 11, Session No. 84. Available online at: <https://gsa.confex.com/gsa/2010AM/webprogram/Paper178221.html> / (accessed on 01 July 2019).
- Hedenquist J.W., Taran Y.A. 2013. Modeling the formation of advanced argillic lithocaps: Volcanic vapor condensation above porphyry intrusions. Economic Geology, 108(7), 1523, Abstract. <https://doi.org/10.2113/econgeo.108.7.1523>
- Hedenquist J.W., Thompson J.F.H., Goldfarb R.J., Richards J.P. (eds.). 2005. Economic Geology: One Hundredth Anniversary Volume: 1905-2005. Littleton, Colorado, Society of Economic Geologists, 1136 p. <https://doi.org/10.5382/AV100>
- Hodgson C.J., Lydon J.W. 1977. The geological setting of volcanogenic massive sulphide deposits and active hydrothermal systems: Some implications for exploration. Canadian Institute of Mining and Metallurgy Bulletin, 70(786), 95-106.
- Horton Jr. W. 1989. Kyanite and sillimanite in high-alumina quartzite of the Battleground Formation, Kings Mountain belt. In: Gair J.E. (ed.) Mineral resources of the Charlotte 1°x2° Quadrangle, North Carolina and South Carolina. U. S. Geological Survey Professional Paper, 1462, 107-110. Available online at: <https://pubs.usgs.gov/pp/1462/report.pdf> / (accessed on 01 July 2019).
- Höy T. 1995. Noranda/Kuroko Massive Sulphide Cu-Pb-Zn. In: Lefebure D.V., Ray G.E. (eds.). 1995. Selected British Columbia Mineral Deposit Profiles: volume 1: Metallics and Coal. British Columbia Ministry of Energy, Mines and Petroleum Resources, Open File 1995-20. p. 53-54. Available online at: http://cmscontent.nrs.gov.bc.ca/geoscience/PublicationCatalogue/OpenFile/BCGS_OF1995-20.pdf / (accessed on 29 April 2021)
- Huston D.L. 1999. Stable isotopes and their significance for understanding the genesis of volcanic-hosted massive sulfide deposits: a review. In: Barrie C.T., Hannington M.D. (eds.). Volcanic-associated massive sulfide deposits: processes and examples in modern and ancient settings. Reviews in Economic Geology, 8. Littleton, Colorado, Society of Economic Geologists. p. 157-179. <https://doi.org/10.5382/Rev.08.07>
- Huston D.L. 2000. Gold in Volcanic-hosted massive sulfide deposits: distribution, genesis, and exploration. In: Hagemann S.G., Brown P.E. (eds.). 2000. Gold in 2000. Reviews in Economic Geology, 13. Littleton, Colorado, Society of Economic Geologists. p. 401-426. <https://doi.org/10.5382/Rev.13.12>
- Hutchinson R.W., Spence C.D., Franklin J.M. (eds.). 1982. Precambrian Sulphide Deposits (H.S. Robinson Memorial Volume). Waterloo, Ontario, Geological Association of Canada Special Paper 25, 791 p.
- Ihlen P.M. 2000. Utilisation of sillimanite minerals, their geology, and potential occurrences in Norway – an overview. Norges Geologiske Undersøkelse Bulletin, NGU-BULL., 436, 113-128. Available online at: https://www.ngu.no/filearchive/102/Bulletin436_12.pdf / (accessed on 23 February 2018).
- Jébrak M., Marcoux É. 2014. Mineral deposit typology. In: Jébrak M.,

- Marcoux É. Geology of Mineral Resources. St. John, Newfoundland Geological Association of Canada, Department of Earth Sciences. p. 41-44.
- Junges S.L., Pimentel M.M., Moraes R. 2002. Nd isotopic study of the Neoproterozoic Mara Rosa Arc, central Brazil: implications for the evolution of the Brasília Belt. *Precambrian Research*, 117(1-2), Abstract. [https://doi.org/10.1016/S0301-9268\(02\)00077-3](https://doi.org/10.1016/S0301-9268(02)00077-3)
- Junges S.L., Pimentel M.M., Dantas E.L., Laux J.H. 2003. New ID-TIMS U-Pb ages in the western portion of the Mara Rosa Arc: Two hundred million years of arc building. *South American Symposium on Isotope Geology*, 4, Volume I, Short Papers, CBPM/IRD, 198-201. Available online at: https://horizon.documentation.ird.fr/exl-doc/pleins_textes/divers17-05/010039206.pdf / (accessed on 20 April 2020).
- Kirkham R.V., Sinclair W.D., Thorpe R.I., Duke J.M. (eds.). 1993. Mineral deposit modeling. Geological Association of Canada Special Paper, 40. Stittsville, Ontario, Geological Association of Canada, 798 p.
- Kuyumjian R.M. 1989a. The geochemistry and tectonic significance of amphibolites from the Chapada sequence, Central Brazil. PhD Thesis, University of London, London, England, 289 p. Available online at: <https://spiral.imperial.ac.uk/bitstream/10044/1/47522/2/Kuyumjian-RM-1989-PhD-Thesis.pdf> / (accessed on 02 Jun 20).
- Kuyumjian R.M. 1989b. Geoquímica e significado do posicionamento geotectônico de rochas plutônicas da região de Chapada, Goiás, Brasil. In: Congresso Brasileiro de Geoquímica, 2, Volume I, Tema II – Litogeoquímica e Geoquímica Isotópica. Rio de Janeiro, SBPq – CPRM/DNPM, 195-201. Available online at: https://3313f8a2-d231-43bd-be73-41e5429b57b2.filesusr.com/ugd/33bad3_5d671023311d4962a2322520cb7a9617.pdf / (accessed on 20 April 2021)
- Kuyumjian R.M. 1991. A suggested hydrothermal exhalative origin for the Chapada copper-gold deposit, Brazil. In: Ladeira E.A. (ed.) *Brazil Gold '91*. Rotterdam, A. A. Balkema, p. p. 231-234.
- Kuyumjian R.M. 1994. Geologia da sequência Mara Rosa na região de Chapada, Goiás. In: Simpósio de Geologia do Centro-Oeste, 4, Brasília, 142-144. Available online at: http://acervo.cprm.gov.br/rpi_cprm/docreaderNET/docreader.aspx?bib=Anais&PagFis=57684 / (accessed on 20 April 2021).
- Kuyumjian R. M. 1995. Diversity of fluids in the origin of the Chapada Cu-Au deposit, Goiás. *Revista Brasileira de Geociências*, 25(3), 203-205. <https://doi.org/10.25249/0375-7536.1995203205>
- Kuyumjian R.M. 1998a. The magmatic arc of western Goiás: A promising exploration target. In: Workshop Depósitos Mineraiis Brasileiros de Metais Base. Salvador, CPGG/UFBA – ADIMB – SBG/BA, 80-85.
- Kuyumjian R.M. 1998b. Kyanite-staurolite ortho-amphibolite from the Chapada region, Goiás, central Brazil. *Mineralogical Magazine*, 62(4), 501-507. <https://doi.org/10.1180/002646198547873>
- Kuyumjian R.M. 2000. Magmatic arc and associated gold, copper, silver, and barite deposits in the state of Goiás, central Brazil: Characteristics and speculations. *Revista Brasileira de Geociências*, 30(2), 285-288. <https://doi.org/10.25249/0375-7536.2000302285288>
- Kuyumjian R.M., Oliveira C.G., Oliveira F.B., Borges C.E.P. 2010. Depósito de Cu-Au porfírico Chapada, Goiás. In: Brito R.S.C., Silva M.G., Kuyumjian R.M. (eds.) *Modelos de depósitos de cobre do Brasil e sua resposta ao intemperismo*. Brasília, CPRM. p. 51-69. Available online at: <http://rigeo.cprm.gov.br/jspui/handle/doc/16979> / (accessed on 20 April 2021)
- Large R.R. 1992. Australian volcanic-hosted massive sulfide deposits: features, styles, and genetic models. *Economic Geology*, 87(3), 471-510. <https://doi.org/10.2113/gsecongeo.87.3.471>
- Laux J.H., Pimentel M.M., Dantas E.L., Armstrong R., Junges S.L. 2005. Two Neoproterozoic crustal accretion events in the Brasília Belt, Central Brazil. *Journal of South American Earth Sciences*, 18(2), Abstract. <https://doi.org/10.1016/j.jsames.2004.09.003>
- Lefebvre D.V., Höy, T. (eds.). 1996. Selected British Columbia mineral deposit profiles: volume 2: Metallic Deposits. British Columbia Ministry of Employment and Investment, Open File 1996-13, 172 p. Available on line at: http://cmscontent.nrs.gov.bc.ca/geoscience/PublicationCatalogue/OpenFile/BCGS_OF1996-13.pdf / (accessed on 29 April 2021)
- Lefebvre D.V., Ray G.E. (eds.). 1995. Selected British Columbia Mineral Deposit Profiles: volume 1: Metallics and Coal. British Columbia Ministry of Energy, Mines and Petroleum Resources, Open File 1995-20, 136 p. Available on line at: http://cmscontent.nrs.gov.bc.ca/geoscience/PublicationCatalogue/OpenFile/BCGS_OF1995-20.pdf / (accessed on 29 April 2021)
- Markham N.L. 1968. Some genetic aspects of the Mt. Lyell mineralization. *Mineralium Deposita*, 3, 199-221. <https://doi.org/10.1007/BF00207434>
- Martini S.L. 2002. Para cada depósito um possível tipo adequado: comparação entre conceitos, atributos e tipos de depósitos metálicos das classificações dos serviços geológicos do Canadá, dos Estados Unidos e da Colúmbia Britânica. Rio de Janeiro, CPRM, 20 p. Available online at: http://acervo.cprm.gov.br/rpi_cprm/docreaderNET/docreader.aspx?bib=DiversosCPRM&PagFis=18301 / (accessed on 20 May 2019)
- Mindat.org. 2019. Prince Lyell Mine, Mount Lyell Mines, Queenstown district, West Coast municipality, Tasmania, Australia. Available online at: <https://www.mindat.org/loc-18798.html> / (accessed on 23 May 2019).
- Miranda H.M., Moore C.M., Patel A., Pignatari L.E.C. 2018. Yamana Gold Inc.: technical report on the Chapada mine, Goiás state, Brazil: NI 43-101 Report. Geological setting and mineralization, p. 7.1-7.18. Deposit types, p. 8.1-8.6. Available online at: <https://www.sedar.com/GetFile.do?lang=EN&docClass=24&issuerNo=0003801&issuerType=03&projectNo=02749702&docId=4285949> / (accessed on 11 May 2021).
- Moore C.M., Miranda H.M., Hampton A.P., Ritchie D.G. 2019. Lundin Mining Corporation: technical report on the Chapada mine, Goiás state, Brazil – NI 43-101 Report. Geological setting and mineralization, p. 7.1-7.25. Deposit types, p. 8.1-8.4. Available online at: https://www.lundinmining.com/site/assets/files/7957/191010_-_chapada_ni_43-101_techncial_report.pdf / (accessed on 11 October 2019).
- Morton J.L., Franklin J.M. 1987. Two-fold classification of Archean volcanic-associated massive sulfide deposits. *Economic Geology*, 82(4), 1057-1063. <https://doi.org/10.2113/gsecongeo.82.4.1057>
- Moura F.G., Oliveira C.G., Giustina M.E.S.D. 2015. Geocronologia de rutilo aplicada ao estudo do depósito de Cu-Au de Chapada. *Simpósio de Geologia do Centro-Oeste*, 14, 64-65. Available online at: http://sbq.sitepessoal.com/anais_digitalizados/simposiocentrooeste/2015.pdf / (accessed on 05 May 2020).
- Müller A., Ihlen P.M., Wanvik J.E., Flem B. 2007. High-purity quartz mineralisation in kyanite quartzites, Norway. *Mineralium Deposita*, 42, 523, Abstract. <https://doi.org/10.1007/s00126-007-0124-8>
- Nascimento E.L.C. 2008. Rochas a cianita-quartzo no Arco Neoproterozoico de Mara Rosa – evidências para mineralização do tipo Cu-Au porfírica. MSc Dissertation, Instituto de Geociências, Universidade de Brasília, Brasília.
- Nascimento E.L.C., Dantas E.L., Oliveira C.G., Allan M. 2008. Kyanite-bearing rocks in the Neoproterozoic Mara Rosa Arc: evidences for Cu-Au porphyry-type mineralization. MSc Dissertation, Instituto de Geociências, Universidade de Brasília, Brasília. Appendix. 55 p.
- Oliveira C.G., Kuyumjian R.M., Oliveira F.B., Marques G.C., Palermo N., Dantas E.L. 2014. Metalogênese do arco magmático de Goiás. In: Silva M.G., Rocha Neto M.B., Jost H., Kuyumjian R.M. (orgs.) *Metalogênese das províncias tectônicas brasileiras*. Brasília, CPRM. p. 455-466. Available online at: <http://rigeo.cprm.gov.br/jspui/handle/doc/19389> / (accessed on 20 April 2021)
- Oliveira C.G., Oliveira F.B., Giustina M.E.S.D., Marques G.C., Dantas E.L., Pimentel M.M., Buhn B.M. 2016. The Chapada Cu–Au deposit, Mara Rosa magmatic arc, Central Brazil: Constraints on the metallogenesis of a Neoproterozoic large porphyry-type deposit. *Ore Geology Reviews*, 72(1), 1-21. <https://doi.org/10.1016/j.oregeorev.2015.06.021>
- Oliveira C.G., Oliveira F.B. Mapa geológico: folha Campinorte SD.22-Z-B-I. Escala 1:100.000. Programa Geologia do Brasil. Brasília, UNB/FINATEC/CPRM, 2007. Available on line at: <http://rigeo.cprm.gov.br/jspui/handle/doc/10425> / (accessed on 20 April 2021).
- Oliveira C.G., Pimentel M.M., Melo L.V., Fuck R.A. 2004. The copper-gold and gold deposits of the Neoproterozoic Mara Rosa magmatic arc, central Brazil. *Ore Geology Reviews*, 25(3-4), 285-299. <https://doi.org/10.1016/j.oregeorev.2004.04.006>
- Oliveira F.B. 2009. Características epigenéticas do depósito de Cu-Au Chapada, arco magmático de Goiás. MSc Dissertation, Instituto de Geociências, Universidade de Brasília, Brasília, 113 p. Available on line at: <https://repositorio.unb.br/handle/10482/9078> / (accessed on 20 April 2021)
- Owens B.E., Pasek M.A. 2007. Kyanite quartzites in the Piedmont Province of Virginia: evidence for a possible high-sulfidation system. *Economic Geology*, 102(3), 495, Abstract. <https://doi.org/10.2113/gsecongeo.102.3.495>
- Palermo N. 1996a. Le gisement aurifère précambrien de Posse (Goiás,

- Brésil) dans son cadre géologique. PhD Thesis, École Normale Supérieure des Mines de Paris, Paris, 220p.
- Palermo N. 1996b. Identificação de três séries magmáticas na região de Mara Rosa, Goiás. In: Congresso Brasileiro de Geologia, 39, 2, 219-222. Available online at: <http://www.sbgeo.org.br/home/pages/44/> (accessed on 20 April 2021)
- Palermo N., Porto C.G., Costa Jr. C.N. 2000. The Mara Rosa gold district, Central Brazil. *Revista Brasileira de Geociências*, 30(2), 256-260. <https://doi.org/10.25249/0375-7536.2000302256260>
- Paradis S., Bailes A., Galley A., Shaw K. 2002. Large-scale hydrothermal alteration systems, Snow Lake area, Manitoba, Canada. In: Galley A., Bailes A., Haninngton M., Holk G., Katsube J., Paquete F., Paradis S., Santaguida F., Taylor B., Hillary B. 2002. Database for CAMIRO Project 94E07: interrelationships between subvolcanic intrusions, large-scale alteration zones and VMS deposits, Geological Survey of Canada, Open File 4431. p. 281-332. <https://doi.org/10.4095/213755>
- Parr J.M., Plimer I.R. 1993. Models for Broken Hill-type lead-zinc-silver deposits. In: Kirkham R.V., Sinclair W.D., Thorpe R.I., Duke J.M. (eds.). 1993. Mineral deposit modeling. Geological Association of Canada Special Paper, 40. Stittsville, Ontario, Geological Association of Canada. p. 253-288.
- Pimentel M.M., Fuck R.A. Jost H., Ferreira Filho C.F., Araújo S.M. 2000. The basement of the Brasília Fold Belt and the Goiás Magmatic Arc. In: Cordani U.G., Milani E.J., Thomaz Filho A., Campos D.A. (eds.). Tectonic Evolution of South America. Rio de Janeiro, International Geological Congress, 31, 195-229. <http://rigeo.cprm.gov.br/jspui/handle/doc/19419>
- Pimentel M.M., Fuck R.A., Machado N., Fuck R.F., Ribeiro K.R., Viana M.G. 1993. Dados geocronológicos U-Pb preliminares da região de Mara Rosa, Goiás: implicações para a época de mineralização de Au e para a evolução tectônica Neoproterozóica no Centro-Oeste. In: Congresso Brasileiro de Geoquímica, 4, 255-258. Available online at: <https://www.sbgq.org.br/anais-dos-congressos/> (accessed on 12 April 2021).
- Pimentel M.M., Jost H., Fuck R.A. 2004. O embasamento da Faixa Brasília e o Arco Magmático de Goiás. In: Mantesso Neto V., Bartorelli A., Carneiro C.D.R., Neves B.B.B. (orgs.). Geologia do Continente Sul-Americano: evolução da obra de Fernando Flávio Marques de Almeida. São Paulo, Editora Beca. p. 355-368.
- Pimentel M.M., Whitehouse M.J., Viana M.G., Fuck R.A., Machado N. 1997. The Mara Rosa Arc in the Tocantins Province: further evidence for Neoproterozoic crustal accretion in central Brazil. *Precambrian Research*, 81(3-4), 299-310. [https://doi.org/10.1016/S0301-9268\(96\)00039-3](https://doi.org/10.1016/S0301-9268(96)00039-3)
- Plimer I.R. 1986. Sediment-hosted exhalative Pb-Zn deposits – Products of contrasting ensialic rifting. *Transactions Geological Society of South Africa*, 89, 57-73. Available online at: <https://pubs.geoscienceworld.org/gssa/sajg/article-standard/89/1/57/122053/Sediment-hosted-exhalative-Pb-Zn-deposits-products>
- Pöll J.S. 1994. The geology of the Zacarias gold-silver-barite deposit, Goiás State, Brazil. MSc Dissertation, Colorado School of Mines, Denver, 124 p. Available on line at: <https://hdl.handle.net/11124/172062/> (accessed on 20 April 2021)
- Poulsen K.H., Hannington M.D. 1996. Volcanic-associated massive sulphide gold. In: *Geology of Canadian Mineral Deposit Types*. Geology of Canada, 8. Ottawa, Geological Survey of Canada, 183-196. <https://doi.org/10.1130/DNAG-GNA-P1>
- Ramos Filho W.L., Araújo Filho J.O., Kuyumjian R.M. 2003. Características do ambiente estrutural do depósito de Chapada, Goiás. *Revista Brasileira de Geociências*, 33(2), 109-116. <https://www.doi.org/10.25249/0375-7536.2003332109116>
- Ramos Filho W.L., Kuyumjian R.M., Pires A.C B. 2005. The Chapada Cu-Au deposit and guidelines for mineral exploration program in the Goiás Magmatic Arc. *Revista Brasileira de Geociências*, 35(4), 603-605. <https://doi.org/10.25249/0375-7536.200535603605>
- Richardson C.J., Cann J.R., Richards H.G., Cowan J.G. 1987. Metal-depleted root zones of the Troodos ore-forming hydrothermal systems, Cyprus. *Earth Planetary Science Letter*, 84(2-3), 243. [https://doi.org/10.1016/0012-821X\(87\)90089-6](https://doi.org/10.1016/0012-821X(87)90089-6)
- Richardson S.V., Kesler S.E., Essene E.J., Jones L.M. 1986. Origin and geochemistry of the Chapada Cu-Au deposit, Goiás, Brazil: A metamorphosed wall-rock porphyry copper deposit. *Economic Geology*, 81(8), 1884-1898. <https://doi.org/10.2113/gsecongeo.81.8.1884>
- Robb L. 2008. Introduction to ore-forming processes. Blackwell Publishing, Oxford, 373 p.
- Routhier P. 1963. Les gisements métallifères: géologie et principes de recherche. Paris, Masson et Cie, 2 v.
- Routhier P. 1980. Où sont les métaux pour l'avenir? Les provinces métalliques: essai de métallogénie globale. Orléans Cedex, Bureau de Recherches Géologiques et Minières. Mémoire BRGM, 105, 410 p.
- Routhier P. 1983. Where are the metals for the future? The metal provinces: an essay on global metallogeny. Orléans Cedex, Éditions du BRGM, 400p.
- Sangster D.F. 1972. Precambrian volcanogenic massive sulphide deposits in Canada: a review. *Geological Survey of Canada Paper*, 72-22, 44 p. <https://doi.org/10.4095/102291>
- Santaguida F., Gibson D.H., Watkinson D.H., Hannington M.D. 2002. Part I: Semi-conformable epidote-quartz hydrothermal alteration in the central Noranda volcanic complex, Canada: Relationship to volcanic activity and VMS mineralization. In: Galley A., Bailes A., Haninngton M., Holk G., Katsube J., Paquete F., Paradis S., Santaguida F., Taylor B., Hillary B. 2002. Database for CAMIRO Project 94E07: interrelationships between subvolcanic intrusions, large-scale alteration zones and VMS deposits, Geological Survey of Canada, Open File 4431. p. 181-242. <https://doi.org/10.4095/213755>
- Shanks III W.C.P. 2012. Hydrothermal alteration in volcanogenic massive sulfide occurrence model. In: Shanks III W.C.P, Thurston R. (eds.) Volcanogenic Massive Sulfide Occurrence Model - U.S. Geological Survey Scientific Investigations Report 2010-5070-C. p. 169-180. <https://doi.org/10.3133/sir20105070C>
- Sillitoe R.H., Hannington M.D., Thompson J.F.H. 1996. High sulfidation deposits in the volcanogenic massive sulfide environment. *Economic Geology*, 91(1), 204-212. <https://doi.org/10.2113/gsecongeo.91.1.204>
- Silva J.A., Sá J.A.G. 1988. Jazida de cobre de Chapada, Mara Rosa, Goiás. In: Schobbenhaus C., Coelho C.E.S. (coords.) Principais depósitos minerais do Brasil: volume III: metais básicos não-ferrosos, ouro e alumínio. Brasília, DNPM/CVRD. p. 55-60.
- Silva S.B., Walker G., Re E.R., Delboni Jr. H., Contreras R., Petter R. 2011. Chapada Mine and Suruca Project – Goiás State, Brazil – Technical report pursuant to National Instrument 43-101 of the Canadian Securities Administrators prepared for Yamana Gold Inc. *Geology and mineralization*, p. 13-15. Deposit types, p. 51-55. Mineralization, p. 55. Available online at: <https://www.sedar.com/GetFile.do?lang=EN&docClass=24&issuerNo=00003801&issuerType=03&projectNo=01724009&docId=2855554/> (accessed on 04 October 2017).
- Skinner B.J. (ed.). 1981. *Economic Geology: Seventy-Fifth Anniversary Volume: 1905-1980*. Lancaster, Pennsylvania, The Economic Geology Publishing Company, 1136 p. <https://doi.org/10.5382/AV75>
- Slack J.F. 2012. Exhalites. In: Shanks III W.C.P, Thurston R. (eds.) Volcanogenic Massive Sulfide Occurrence Model - U.S. Geological Survey Scientific Investigations Report 2010-5070-C. p. 159-163. <https://doi.org/10.3133/sir20105070C>
- Spry P.G., Peter J.M., Slack J.F. 2000. Meta-exhalites as exploration guides to ore. In: Spry P.G., Marshall B., Vokes F.M. (eds.) *Metamorphosed and Metamorphogenic Ore Deposits*. Reviews in Economic Geology, 11, Chapter 8. Lancaster, Pennsylvania, Society of Economic Geologists. p. 163-201. <https://doi.org/10.5382/Rev.11.08>
- Taylor B. 2007. Epithermal gold deposits. In: Goodfellow W.D. (ed.). *Mineral deposits of Canada: a synthesis of major deposit-types, district metallogeny, the evolution of geological provinces, and exploration methods*. Geological Association of Canada, Mineral Deposits Division and Geological Survey of Canada, Special Publication, 5. p. 113-139.
- Valeriano C.M., Dardenne M.A., Fonseca M.A., Simões L.S.A., Seer J.H. 2004 A evolução tectônica da Faixa Brasília. In: Mantesso-Neto V., Bartorelli A., Carneiro C.D.R., Brito Neves B.B. (orgs.) *Geologia do Continente Sul-Americano: evolução da obra de Fernando Flávio Marques de Almeida*. São Paulo, Editora Beca. p. 575-592.
- Viana M.G., Pimentel M.M., Whitehouse M.J., Fuck R. A., Machado N. 1995. O arco magmático de Mara Rosa, Goiás: geoquímica e geocronologia e suas implicações regionais. *Revista Brasileira de Geociências*, 25(2), 111-123. <https://doi.org/10.25249/0375-7536.1995111123>
- Walford D.C., Franklin J.M. 1982. The Anderson Lake mine, Snow Lake, Manitoba. In: Hutchinson R.W., Spence C.D., Franklin J.M. (eds.) *Precambrian Sulphide Deposits (H.S. Robinson Memorial Volume)*. Waterloo, Ontario, Geological Association of Canada Special Paper 25. p. 481-523.

Walshe J.L., Salomon M. 1981. An investigation into the environment of formation of the volcanic-hosted Mt. Lyell copper deposits using geology, mineralogy, stable isotopes, and a six-component chlorite solid solution model. *Economic Geology*, 76(2), 246, Abstract. <https://doi.org/10.2113/gsecongeo.76.2.246>

Willner A., Shreyer W., Moore J.M. 1990. Peraluminous metamorphic rocks from the Namaqualand Metamorphic Complex (South Africa): Geochemical evidence for an exhalation-related, sedimentary origin in a Mid-Proterozoic rift system. *Chemical Geology*, 81(3), 221, Abstract. [https://doi.org/10.1016/0009-2541\(90\)90117-P](https://doi.org/10.1016/0009-2541(90)90117-P)